Physica D 288 (2014) 1–22

Contents lists available at ScienceDirect

Physica D

journal homepage: www.elsevier.com/locate/physd

Optimal entrainment with smooth, pulse, and square signals in weakly forced nonlinear oscillators

Hisa-Aki Tanaka *

Graduate School of Informatics and Engineering, The University of Electro-Communications, 1-5-1 Chofugaoka, Chofu, Tokyo 182-8585, Japan

HIGHLIGHTS

- We consider the optimization problem maximizing the entrainability of nonlinear oscillators.
- A fundamental limit of entrainment is systematically clarified as follows.
- For 1:1 entrainment, the global optimal forcing is obtained in L^p-space ($p > 1$).
- And, the global optimal pulse-like forcings in L^1-space is obtained.

ARTICLE INFO

Article history:
Received 1 October 2013
Received in revised form
21 June 2014
Accepted 16 July 2014
Available online 14 August 2014
Communicated by Y. Nishiura

Keywords:
Entrainment
Synchronization
Arnold tongue
Optimization
Hölder's inequality

ABSTRACT

A physical limit of entrainability of nonlinear oscillators is considered for an external weak signal (forcing). This limit of entrainability is characterized by the optimization problem maximizing the width of the Arnold tongue (the frequency-locking range versus forcing magnitude) under certain practical constraints. Here we show a solution to this optimization problem, thanks to a direct link to Hölder's inequality. This solution defines an ideal forcing realizing the entrainment limit, and as the result, a fundamental limit of entrainment is clarified as follows. For 1:1 entrainment, we obtain (i) a construction of the global optimal forcing and a condition for its uniqueness in L^p-space with $p > 1$, and (ii) a construction of the global optimal pulse-like forcings in L^1-space, and for m:n entrainment ($m \neq n$), some informations about the non-existence of the ideal forcing. (iii) In addition, we establish definite algorithms for obtaining the global optimal forcings for $1 < p \leq \infty$ and these pulse-like forcings for $p = 1$. These theoretical findings are verified by systematic, extensive numerical calculations and simulations.

© 2014 The Author. Published by Elsevier B.V.
This is an open access article under the CC BY-NC-ND license (http://creativecommons.org/licenses/by-nc-nd/3.0/).

1. Introduction

Entrainment of nonlinear oscillators (limit-cycle oscillators) to an external forcing is a fundamental phenomenon of wide interest with a long history and a large variety of applications [1]. Such entrainment emerges in nonlinear oscillators, which adjust their frequencies to that of an external forcing above a critical forcing amplitude. In biology, circadian rhythm control [2] and exogenous pace-maker control of the heart [3] by entrainment have been well documented, and recent findings have revealed an entrainment mechanism in insects as well, in particular with respect to auditory sensitivity and selectivity of mosquitoes [4]. At the same time, entrainment to sinusoidal forcing in the field of engineering has been well known for many years, as described by van der Pol [5] and Adler [6], where entrainment is referred to as injection-locking. Recently, in addition to the classical setting of using sine wave inputs to oscillators, numerous cases of using a non-sinusoidal input to oscillators have been described [7–9]. Since entrainment is technologically feasible without any additional circuitry, the need for a high-frequency, low-power consumption injection-locked oscillator has garnered widespread attention for this classical technology in recent years. For instance, there have been many studies related to engineering oscillator entrainment, particularly in the fields of microelectronics and nano-electromechanical systems [7–12].

An Arnold tongue, which shows the region where entrainment has been realized (*i.e.*, the locking range) in a forcing amplitude versus forcing frequency diagram, is important for indexing entrainability, particularly with the injection-locking technique. Hence, in many areas, the Arnold tongue is used for measuring entrainability [1]. In its most common situation, entrainment adjusts the oscillation frequency of a nonlinear oscillator to that of an external forcing and the ratio of the two frequencies becomes exactly 1:1

* Tel.: +81 42 443 5174; fax: +81 42 443 5174.
E-mail address: htanaka@uec.ac.jp.

http://dx.doi.org/10.1016/j.physd.2014.07.003
0167-2789/© 2014 The Author. Published by Elsevier B.V. This is an open access article under the CC BY-NC-ND license (http://creativecommons.org/licenses/by-nc-nd/3.0/).

(*i.e.*, 1:1 entrainment). In addition to this 1:1 entrainment, the more general m:n (*i.e.*, m:n entrainment) is often observed for this ratio in a narrower Arnold tongue [4,7,13]. For instance, in the case of m:1 entrainment, the utility value is high where the injection-locking technique is required, because it is possible to decrease the phase noise, stabilizing the oscillating frequency of a high-frequency oscillator, simply by injecting $1/m$ low-frequency forcing, which is relatively easily generated [7].

The nature of entrainment and entrainment processes, as typified by an Arnold tongue, can be described by the so-called phase equation as being under a weak forcing limit, as in the case in Section 2 below [14,15]. This description method may be one of the most successful description methods offered to date, given its universality and applicability, as long as the forcing is not strong. (Historically, this phase equation is deemed as a natural generalization of the well-known Adler's equation [6] for sinusoidal forcing.) For example, the nature of an Arnold tongue of m:n entrainment has been analyzed using this phase equation [15], and we will also conduct our analysis using this phase description.

As stated above, knowledge about entrainment has become more multifaceted and more accurate over time, and practical application is also becoming important. However, the notion of a physical limit of this nonlinear phenomenon is still undeveloped. In recent years, there have been studies aimed at engineering entrainment with an optimal input (forcing). These include studies related to the determination of the optimal input for the establishment of fast entrainment [16,17], circadian phase resetting [18,19], the starting and stopping of oscillations [19,20], and maximal resonance (energy transfer) between a system and a forcing signal [21]. Control of deterministic [8,22] and stochastic [23,24] neuronal spiking activity has been achieved with the use of a phase description approach combined with variational methods for optimization of spiking time or the variance of firing rates. In addition to these accomplishments, it has become possible to characterize the minimal power forcing waveform that produces the largest locking range of nonlinear oscillators through the use of variational calculus [25]. However, currently, knowledge is lacking with respect to the existence of a physical limit in relation to several problems of entrainment, for example, whether it is possible to answer the following basic questions:

Q1 Does a power-reduced forcing (*e.g.*, periodic injection current with a limited squared average of its waveform, if the forcing is given as a current) that produces the largest locking range for 1:1 entrainment exist for a given limit cycle oscillator? If it exists, is it uniquely obtained? Or is there a definitive algorithm for finding it?

Q2 Is 'the largest locking range' as mentioned in **Q1** also feasible if an area-reduced forcing (*e.g.*, injection current with limited total absolute value of its waveform) or a magnitude-reduced forcing (*e.g.*, injection current with limited amplitude) is considered?

A common thread connecting the above questions is relevant to the fundamental limit of entrainment; if the existence of a hidden simple mathematical structure were uncovered, then the questions **Q1** and **Q2** could be answered in a unified and transparent manner. In the present paper, we demonstrate such a hidden structure, supported by theory and systematic simulations.

2. Basic definitions

The entrainment process of a limit-cycle oscillator in the weak forcing limit can be modeled by

$$\frac{d\psi}{dt} = \omega + \epsilon Z(\psi) f(\Omega t), \tag{1}$$

where ψ is the phase variable of the oscillator ($\psi \in [-\pi, \pi] \equiv S$), Z is the phase response (sensitivity) function, and ω and Ω are the natural frequency of the oscillator and the frequency of the weak forcing $\epsilon f(\Omega t)$, respectively, following the notation in [14]. In general, m:n entrainment occurs when $\frac{\omega}{m} \sim \frac{\Omega}{n}$ is satisfied for positive relatively prime integers m and n. In this situation, Eq. (1) is further simplified by the method of averaging (and after setting ϵ to 1) to

$$\frac{d\phi}{dt} = \Delta\omega + \Gamma_{m/n}(\phi), \tag{2}$$

where ϕ and $\Delta\omega$ satisfy $\phi = \psi - \frac{m}{n}\Omega t$ and $\Delta\omega = \omega - \frac{m}{n}\Omega$, respectively, and the interaction function $\Gamma_{m/n}(\phi)$ is determined by f and Z as

$$\begin{aligned}\Gamma_{m/n}(\phi) &= \frac{1}{T}\int_0^T Z\left(\frac{m}{n}\Omega t + \phi\right) f(\Omega t)dt \\ &= \frac{1}{2\pi}\int_{-\pi}^{\pi} Z(m\theta + \phi) f(n\theta)d\theta \\ &\equiv \frac{1}{2\pi}\left\langle Z(m\theta + \phi) f(n\theta)\right\rangle, \end{aligned} \tag{3}$$

in which $T = \frac{2\pi n}{\Omega}$ (n times the natural period of the oscillator), and $\theta \in [-\pi, \pi]$ represents $\frac{\Omega t}{n}$. When considering the case of $m = n = 1$, *i.e.*, $1:1$ entrainment, we will abbreviate $\Gamma_{m/n}$ as Γ, for simplicity. We note that in [15] Eq. (2) is also derived as a direct consequence of Malkin's theorem.

We consider a general class of periodic functions $f(\theta)$ as the weak forcing, namely those satisfying the following constraint:

$$\|f\|_p \equiv \left\langle |f(\theta)|^p \right\rangle^{\frac{1}{p}} = M, \tag{4}$$

in which both p and M are positive constants; here we assume $f \in L^p(S)$, namely that f is an L^p-function on $S \equiv [-\pi, \pi]$. In this paper, we assume $p \geq 1$, due to the following physical interpretation of the constraint (4). First, for $p = 2$, Eq. (4) is equivalent to simply $\langle f^2 \rangle = M^2$, *i.e.*, the squared average (the power) of f is fixed at M^2, which is the case considered in [25], and this case corresponds to the power-reduced forcing in **Q1** given in Section 1. For $p = 1$, Eq. (4) corresponds to the area-reduced forcing in **Q2**: $\left\langle |f(\theta)| \right\rangle = M$. On the other hand, for $p = \infty$, Eq. (4) implies the magnitude-reduced forcing in **Q2**, because $\|f\|_\infty = M$: $|f(\theta)| \leq M$ for a.e. $\theta \in S$, since $\|f\|_\infty$ is the essential supremum of $|f(\theta)|$. Thus, the constraint (4) continuously covers various situations in a natural way.

In addition to Eq. (4), another constraint,

$$\frac{1}{2\pi}\left\langle f(\theta)\right\rangle = 0, \tag{5}$$

i.e., a charge-balance constraint [8], is introduced here, because it is required in practical situations where total injection (injected current) should be 0.

Now, the entrained, frequency- and phase-locked states of the forcing f are characterized as stable fixed points in Eq. (2), and the following properties of (i) and (ii) are equivalent:

(i) Eq. (2) has a stable fixed point at $\phi = \phi_*$.

(ii) $\Delta\omega + \Gamma(\phi_*) = 0$ and $\Gamma'(\phi_*) < 0$.

If we change the value of $\Delta\omega$ in (ii), a maximal interval $(\Delta\omega_+, \Delta\omega_-)$ is defined where a stable fixed point ϕ_* exists, as shown in Fig. 1; here a generic situation is assumed, in which $\Gamma(\phi)$ attains a unique maximum and a unique minimum respectively at $\phi = \phi_+$ and $\phi = \phi_-$.

Notice, this does not exclude the possibility for multiple optima of Γ. By $\Delta\omega_\pm + \Gamma(\phi_\pm) = 0$ and $\Gamma(\phi_+) > \Gamma(\phi_-)$, the maximum minus the minimum of $\Gamma(\equiv \Gamma(\phi_+) - \Gamma(\phi_-))$ defines the width of entrainable frequency detuning $\Delta\omega \equiv \Delta\omega_+ - \Delta\omega_- > 0$,

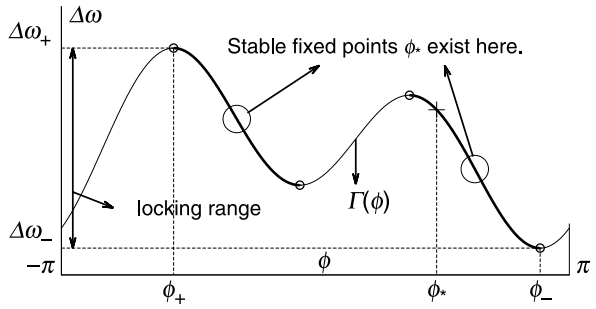

Fig. 1. Locking range $\Delta\omega_+ - \Delta\omega_- \ (=\Gamma(\phi_+) - \Gamma(\phi_-) \equiv R[f])$ for generic Γ.

i.e., the locking range, for which the phase-locked state is stably maintained.

Thus, the functional

$$R[f] = \Gamma(\phi_+) - \Gamma(\phi_-) = \frac{1}{2\pi}\left\langle Z(\theta+\phi_+)f(\theta) - Z(\theta+\phi_-)f(\theta)\right\rangle \tag{6}$$

is defined, indicating the width of the locking range for given f and Z. Then, for maximizing $R[f]$ under the constraint (5), the functional

$$J[f] = R[f] + \frac{\lambda}{2\pi}\left\langle f(\theta)\right\rangle \tag{7}$$

is naturally introduced, where λ is a Lagrange multiplier. Regarding this optimization problem of $J[f]$, the following questions are of fundamental interest, besides being important for practical applications, as mentioned in Section 1. First, does this optimization problem have any solution? If so, how can we find the best solution? Namely, can we find all (possibly multiple) locally optimal solutions and can we distinguish the best one among them? Some of these questions are answered in the affirmative, and such optimization problems can be solved in a unified way, as shown below.

3. Main results

In Refs. [8,9,17,25], optimal forcings have been designed for various purposes and constraints. Their arguments are all based on variational calculus, such as the Euler–Lagrange equation [26] or Pontryagin's minimum principle [27]. These frameworks generally provide wide applicability for problems beyond the particular entrainment problem we pose in Section 2. However, they have a limitation: they are intrinsically local and heuristic, and their results lack global information. Hence, by using only variational calculus, it is hard to answer the questions of **Q1** and **Q2** posed in Section 1 regarding global information of all possible optimal forcings. The purpose of the present paper is to show that these questions are answered in a definite way for a certain general class of limit-cycle oscillators:

S1 For 1:1 entrainment under the constraints (4) and (5) with $1 < p < \infty$, the global optimal solution to the functional (7) is explicitly obtained in $L^p(S)$, if it exists. Namely, its waveform is given by a closed formula of Z (through Eqs. (57), (62) and (63)). Thus, **Q1** is answered in the affirmative (as the special case of $p = 2$).

S2 For the same 1:1 entrainment optimization with $p = 1$, a unique upper limit of (7) (*i.e.*, an ideal locking range) exists for some generic Z, and this limit is asymptotically realized by a particular pair of one positive pulse and one negative pulse in $L^1(S)$, which is consistent with the result of **S1** in the limit of $p \to 1$. On the other hand, for $p = \infty$, the global optimal solution to the 1:1 entrainment optimization is explicitly obtained in $L^\infty(S)$ if it exists, and its closed formula is given in terms of Z (which resembles the well-known bang–bang principle [27]). Again, this is consistent with the limit of $p \to \infty$ in **S1**. These results give positive solutions to **Q2**.

The statements in **S1** and **S2** are consequences of four theorems presented in Section 5. Some examples of resulting best forcings (*i.e.*, the global optimal forcing $f_{\mathrm{opt},\,p}$ defined by Eqs. (26) and (32) in Section 5) for the Hodgkin–Huxley neuron model [17,28] are shown in Fig. 2 for the cases of $p = 1,\ 2$, and $p = \infty$.

4. Some properties derived from Hölder's inequality in preparation for later analysis

Here we focus on the well-known Hölder's inequality (*i.e.*, Theorem 3.5 in [29] for measurable functions and Theorem 3.8 in [29] for functions of $f \in L^p(S)$ and $g \in L^q(S)$) in preparation for the analysis in Section 5. Hölder's inequality is stated as follows:

$$\|fg\|_1 \le \|f\|_p \|g\|_q, \tag{8}$$

for p and q satisfying $1 \le p, q \le \infty$ and $p^{-1} + q^{-1} = 1$. For $1 < p, q < \infty$, the equality in (8), (*i.e.*, $\|fg\|_1 = \|f\|_p\|g\|_q$), holds if and only if there exist constants r and s, not both 0, such that $r|f(\theta)|^p = s|g(\theta)|^q$ (a.e. on S). Hereinafter, we call this simply the *equality condition*.

From the setting in Section 2, f in the inequality (8) is now regarded as the forcing waveform f in Eq. (1). Thus, the functional $J[f]$ in Eq. (7) is related to Hölder's inequality by plugging the constraint (4) into (8):

$$2\pi \cdot J[f] = \langle (Z(\theta+\phi_+) - Z(\theta+\phi_-) + \lambda) f(\theta)\rangle \equiv \langle fg\rangle \le \langle |fg|\rangle = \|fg\|_1 \le \|f\|_p\|g\|_q = M\|g\|_q, \tag{9}$$

where $g(\theta) \equiv Z(\theta+\phi_+) - Z(\theta+\phi_-) + \lambda$, and $q = \frac{p}{p-1}$. The constraints in Eq. (9) imply that there exists an upper bound of $J[f]$, *i.e.*, the *ideal* locking range $R[f]$ under the constraints of (4) and (5). In addition, for the case of $1 < p < \infty$ mentioned above, the *equality condition* has to be satisfied for this *ideal* locking range to be realized. Furthermore, for any given g, it is possible to construct optimal f satisfying the *equality condition* $r|f(\theta)|^p = s|g(\theta)|^q$ as follows:

$$|f(\theta)| = \left(\frac{s}{r}\right)^{\frac{1}{p}} |g(\theta)|^{\frac{1}{p-1}} > 0, \quad \text{or equivalently}$$

$$f(\theta) = \sigma(\theta)\left(\frac{s}{r}\right)^{\frac{1}{p}} |g(\theta)|^{\frac{1}{p-1}}, \tag{10}$$

where $\sigma(\theta)$ denotes any function having either ± 1 values for $\theta \in S$. (In Section 8.3, this $\sigma(\theta)$ is again used.) Notice, $(s/r)^{1/p}$ in Eq. (10) is given by

$$\left(\frac{s}{r}\right)^{\frac{1}{p}} = \frac{\|f\|_p}{\|g\|_q^{\frac{q}{p}}} = \frac{M}{\|g\|_q^{\frac{1}{p-1}}}, \tag{11}$$

since $r\|f\|_p^p = s\|g\|_q^q \ne 0$. Thus, Eqs. (10) and (11) result in a convenient form:

$$f(\theta) = M\sigma(\theta)\left(\frac{|g(\theta)|}{\|g\|_q}\right)^{\frac{1}{p-1}}. \tag{12}$$

This form becomes a basic component for constructing *ideal* solutions in Sections 4.1 and 4.2.

Below, we start from the case of $1 < p < \infty$ in Section 4.1. Next, we separately consider the two limits $p \to \infty$ and $p \to 1$ in Section 4.2. Finally, we verify their consistency with the cases of $p = \infty$ and $p = 1$, respectively, in Sections 4.3 and 4.4.

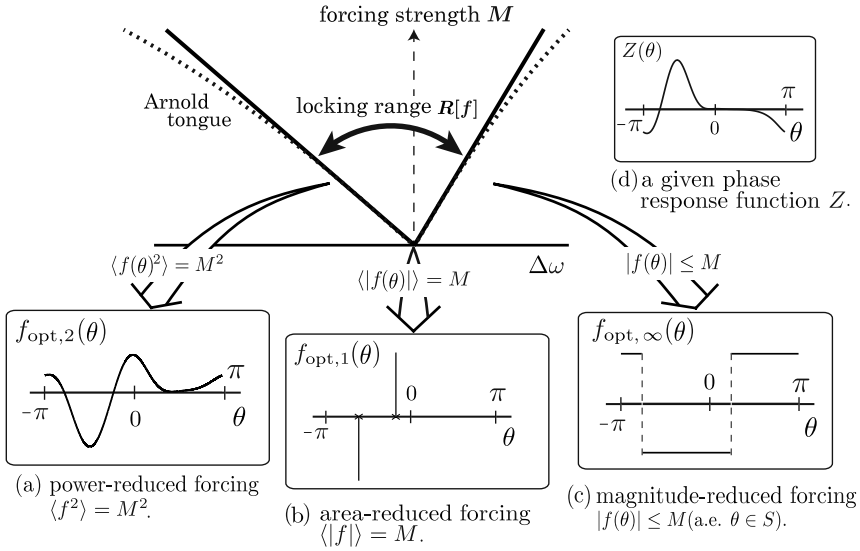

Fig. 2. Global optimal forcings maximizing the range of entrainment: (a) power-reduced forcing in **Q1**, (b) area-reduced forcing in **Q2**, and (c) magnitude-reduced forcing in **Q2**, obtained for (d) the phase response function from the Hodgkin–Huxley phase model [17,28]. Here $f_{\mathrm{opt},\,p}$ ($p = 1, 2$, and ∞) is defined by Eqs. (26) and (32) in Section 5.

4.1. Case of $1 < p < \infty$

First, an *ideal* solution is constructed from the building component (12), as follows.

Lemma 1. *For $f \in L^p(S)$ and $g \in L^q(S)$, suppose that $\|g\|_q$ is a constant, having a value independent of the choice of f. Then, a necessary condition for f to maximize $J[f]$ is uniquely given by the following:*

$$f_{*,\,p}(\theta) = \left\{ \begin{array}{ll} M\left(\dfrac{|g(\theta)|}{\|g\|_q}\right)^{\frac{1}{p'}}, & \text{for } g(\theta) \ge 0 \\ -M\left(\dfrac{|g(\theta)|}{\|g\|_q}\right)^{\frac{1}{p'}}, & \text{for } g(\theta) \le 0 \end{array} \right\}$$

$$= M\mathrm{sgn}[g(\theta)]\left(\frac{|g(\theta)|}{\|g\|_q}\right)^{\frac{1}{p'}}, \tag{13}$$

where $p' = p - 1$.

Hereafter, we call this solution (13) as an ideal *solution since it realizes a possible* ideal *entrainment of the maximum locking range. The proof of this lemma is given in Section 8.1. Note that, in Lemma 1 and its proof, we do not assume that the prime periods of f and g are necessarily the same; their ratio can be m: n in general, and this amounts to the case of m: n entrainment. Then, in such general m: n entrainment, the question is whether the* ideal *solution of Eq. (13) is indeed realized. A negative answer is obtained as follows.*

Lemma 2. *For $f \in L^p(S)$ and $g \in L^q(S)$, the* ideal *solution $f_{*,\,p}$ in Eq. (13) cannot exist in $L^p(S)$ if $m \neq n$.*

The proof of this lemma is given in Section 8.2. Although this shows a somewhat negative property for the general $m \neq n$ case, it is possible to construct (not the ideal*, but) a certain optimal solution if we impose some additional assumptions on f and g, which is reported in another paper* [30].

4.2. Limiting cases of $p \to \infty$ and $p \to 1$

As a natural extension of the results in Section 4.1, here both limits of Eq. (13), $p' \to \infty$ ($p = p' + 1 \to \infty$) and $p' \to +0$ ($p = p' + 1 \to 1$), are considered. In the context of the optimization problem posed in Section 2, as g is explicitly given by Z (through Eqs. (57), (62), and (63) in Section 5.1), the following assumption is natural:

$$0 < \|g\|_q < \infty \quad \text{and} \quad 0 \le |g(\theta)| < \infty, \quad \forall\theta \in S. \tag{14}$$

Given this assumption, direct calculations lead to the following lemma, as proved in Section 8.3.

Lemma 3. *For $f_{*,\,p}$ given by Eq. (13) and $g \in L^q(S)$ satisfying Eq. (14), as $p \to \infty$,*

$$f_{*,\,p}(\theta) \to M\mathrm{sgn}[g(\theta)], \quad \textit{pointwise for } \forall\theta \in S \tag{15}$$

and as $p \to 1$,

$$f_{*,\,p}(\theta) \to \begin{cases} 0, & \textit{pointwise for } \theta \neq \theta_* \\ +\infty, & \text{for } \theta = \theta_* \text{ with } g(\theta_*) > 0 \\ -\infty, & \text{for } \theta = \theta_* \text{ with } g(\theta_*) < 0 \end{cases} \tag{16}$$

where θ_* represents a maximal point of $|g(\theta)|$ in S.[1]

In Sections 4.3 and 4.4, the result in Lemma 3 is reconsidered for the cases of $p = \infty$ and $p = 1$, respectively.

4.3. Case of $p = \infty$

First, we begin with the case of $p = \infty$; Hölder's inequality (8) for $(p, q) = (\infty, 1)$ becomes

$$\|fg\|_1 \le \|f\|_\infty \|g\|_1 = M\|g\|_1 \tag{17}$$

after plugging in the constraint $\|f\|_\infty = M$. This implies that the *ideal* solution f maximizing $\|fg\|_1$ for a given constant $\|g\|_1$ satisfies $\|f_{*,\,\infty}\, g\|_1 = M\|g\|_1$, and from this *ideal* solution $f_{*,\,\infty}$ is easily found:

$$f_{*,\,\infty}(\theta) = M\mathrm{sgn}[g(\theta)], \quad \text{a.e. on } S \tag{18}$$

which is consistent with the limit shown in Eq. (15) obtained as $p \to \infty$ in Section 4.2. The optimality and unique representation of this solution is guaranteed as follows.

[1] Here we have assumed that the maximal points have measure 0 in S. However, even if these points have finite measure, *i.e.*, there exists some interval filled with these maximal points, we can repeat the same argument as above by replacing $\langle|\bar{g}(\theta)|^{1+\frac{1}{p'}}\rangle^{\frac{1}{1+p'}} \to +0$ with $\langle|\bar{g}(\theta)|^{1+\frac{1}{p'}}\rangle^{\frac{1}{1+p'}} \to$ (measure of such points)$/(2\pi)$. In this case, $f_{*,\,p}(\theta) \to \pm 2\pi M \cdot$ (*measure of such points*)$^{-1}$ for $\theta = \theta_*$, instead of $f_{*,\,p}(\theta) \to \pm\infty$ in Eq. (16).

Lemma 4. *For $f \in L^\infty(S)$ and $g \in L^1(S)$, assume $g(\theta) \neq 0$, a.e. on S. Then, the* ideal *solution $f_{*,\infty}$ defined in Eq. (18) gives the unique maximum of the functional $\|fg\|_1$, and this is true only for 1:1 entrainment.*

The proof of this lemma is given in Section 8.4, where we resort to direct verification of the unique representation of $f_{*,\infty}$, since the Hölder's inequality cannot hold with equality in the case of $p = \infty$.

4.4. Case of $p = 1$

Next, we consider the case of $p = 1$. In contrast to the case of $p = \infty$ in Eq. (17), Hölder's inequality for $(p, q) = (1, \infty)$ becomes

$$\|fg\|_1 \leq \|f\|_1 \|g\|_\infty = M\|g\|_\infty, \tag{19}$$

under the constraint $\|f\|_1 = M$. In this case, f can have an arbitrarily tall, pulse-like shape; this is not always allowed in the previous cases of $1 < p \leq \infty$. For instance, if we consider a square waveform with its height $= \epsilon^{-1}$ and its width $= \epsilon$, the constraint $\|f\|_p = \epsilon^{1-p}$ becomes unboundedly large as f becomes more pulse-like.

Now, suppose that an *ideal* solution $f_{\text{ideal},\,1}(\theta)$ having non-zero values on an interval $I \equiv [a, b] \subset S$ (and $f_{\text{ideal},\,1}(\theta) \equiv 0$ on $S \setminus I$) exists, which realizes the *ideal* locking range, *i.e.,*

$$\langle f_{\text{ideal},\,1}\, g\rangle = \|f_{\text{ideal},\,1}\, g\|_1 = \|f_{\text{ideal},\,1}\|_1 \|g\|_\infty = M\|g\|_\infty. \tag{20}$$

However, such $f_{\text{ideal},\,1}$ cannot exist in $L_1(S)$ for a given generic g under certain natural conditions. The proof of this property is given in Appendix A.

Thus, instead of seeking such an $f_{\text{ideal},\,1}$ that realizes the *ideal* locking range, here we design $f_{*,\,1}$ having non-zero values on certain intervals such that the locking range of $f_{*,\,1}$ becomes arbitrarily close to the ideal one, *i.e.*, $f_{*,\,1}$ realizes $\langle f_{*,\,1}\, g\rangle = \|f_{*,\,1}\, g\|_1 \to M\|g\|_\infty$, as the total length of the intervals ($=O(\epsilon)$) of $f_{*,\,1}$ goes to $+0$. One such instance of $f_{*,\,1}$ is given, referring to the limit Eq. (16) in Lemma 3, by

$$f_{*,\,1}(\theta) = M \sum_{i=1}^{n} \text{sgn}[g(\bar\theta_i)]\Delta(\theta - \bar\theta_i). \tag{21}$$

Here we assume that multiple maxima $\bar\theta_i$ of $|g(\theta)|$ exist, *i.e.*, $|g(\bar\theta_i)| = |g(\bar\theta_j)|$ for $1 \leq i, j \leq n$, with n being the number of $\bar\theta_i \in S$, and $|g(\bar\theta_i)| = |g(\bar\theta_j)| > |g(\theta)|$ for any θ except for $\bar\theta_{i,\,j}$. The function $\Delta(\theta - \bar\theta_i)$ is defined by

$$\Delta(\theta - \bar\theta_i) = \begin{cases} \dfrac{1}{2n\epsilon}, & \text{for } |\theta - \bar\theta_i| \leq \epsilon \\ 0, & \text{otherwise.} \end{cases} \tag{22}$$

With these definitions, the following lemma is obtained (the proof is given in Section 8.5). Note, a natural example of the case of $n = 2$, having two distinct $\bar\theta_1$ and $\bar\theta_2$, appears in Section 5.3, although this multiple maxima seems a bit artificial at this stage.

Lemma 5. *For $f \in L^1(S)$ and $g \in L^\infty(S)$, if $|g(\theta)|$ has multiple isolated maximal points $\bar\theta_i$, i.e., there exist $i_1 \neq i_2$ such that $|g(\bar\theta_{i_1})| = |g(\bar\theta_{i_2})|$ are maximal, and if $g(\theta)$ is continuous at each $\bar\theta_i$, then $f = f_{*,\,1}$ in Eq. (21) realizes the ideal (largest) value of $\|fg\|_1 = M\|g\|_\infty$ ($2\pi \times$ locking range $R[f]$) as $\epsilon \to 0$.*

5. Optimization of $J[f]$

Having finished the preparations in Section 4, we are now in a position to solve the optimization problem of $J[f]$ posed in Section 2. First, note that Eq. (7), $J[f] = R[f] + \frac{\lambda}{2\pi}\langle f(\theta)\rangle$, can be rewritten as

$$J[f] = R[f] + \frac{\lambda}{2\pi}\langle f(\theta)\rangle = \frac{1}{2\pi}\langle(\bar Z(\theta) + \lambda) f(\theta)\rangle \equiv \frac{1}{2\pi}\langle fg\rangle, \tag{23a}$$

where

$$\bar Z(\theta) = Z(\theta + \Delta\phi) - Z(\theta) \quad \text{and} \quad \Delta\phi \equiv \phi_+ - \phi_-, \tag{23b}$$

after moving to the new coordinate: $\theta + \phi_- \to \theta$. Thus, the optimization of $J[f]$ is identical to the optimization of $R[f]$ under the following constraints: $\langle f(\theta)\rangle = 0$ and $\langle |f(\theta)|^p\rangle^{\frac{1}{p}} = \|f\|_p = M$. Now, in Eq. (23a), $g(\theta)$ is given as

$$g(\theta) = Z(\theta + \Delta\phi) - Z(\theta) + \lambda = \bar Z(\theta) + \lambda. \tag{24}$$

We note, at this stage both $\Delta\phi$ and λ are undetermined free parameters (which should be determined later). Namely, there is no room for g to be affected by f. Thus, the assumption in Lemma 1 that g and $\|g\|_q$ are independent of f is satisfied, and the results of Lemmata 1–5 are applied to this optimization problem. Then, we consider the three cases of $1 < p < \infty$, $p = 1$, and $p = \infty$ separately, where we construct global optimal solutions $f_{\text{opt},\,p}$, $f_{\text{opt},\,\infty}$, and $f_{\text{opt},\,1}$ to $J[f]$, and we determine the associated $(\Delta\phi, \lambda)$ for a given Z, as follows. Hereinafter, we abbreviate $\frac{p'+1}{p'}$ and $\frac{1}{p'}$, respectively, as

$$\alpha \equiv \frac{p'+1}{p'} > 1, \qquad \beta \equiv \frac{1}{p'} > 0, \tag{25}$$

where $p' = p - 1$.

5.1. Case of $1 < p < \infty$

For $1 < p < \infty$ from Lemma 1, the global optimal solution $f_{\text{opt},\,p}$ is constructed from Eq. (13) and $g(\theta) = \bar Z(\theta) + \lambda$:

$$f_{\text{opt},\,p}(\theta) = M\text{sgn}[\bar Z(\theta) + \lambda]\left(\frac{|\bar Z(\theta) + \lambda|}{\|\bar Z(\theta) + \lambda\|_q}\right)^\beta, \tag{26}$$

where $(\Delta\phi,\ \lambda)$ now means some particular constants which should be determined. Namely, we assume such an $f_{\text{opt},\,p}$ to exist, *i.e.*, $(\Delta\phi,\ \lambda)$ exists for a given Z (which is later verified). Then, for any given Z, the optimum of $\langle fg\rangle$ becomes

$$\begin{aligned}\langle f_{\text{opt},\,p}(\theta)\, g(\theta)\rangle &= \|f_{\text{opt},\,p}\|_p \|g\|_q = M\langle|\bar Z(\theta) + \lambda|^q\rangle^{\frac{1}{q}} \\ &= M\langle|\bar Z(\theta) + \lambda|^\alpha\rangle^{\frac{1}{\alpha}}\ (=2\pi J[f_{\text{opt},\,p}]).\end{aligned} \tag{27}$$

In order to maximize $J[f_{\text{opt},\,p}]$, the function $\langle|\bar Z(\theta) + \lambda|^\alpha\rangle$ should be maximized by tuning the two free parameters $\Delta\phi$ and λ in Eq. (23a), since M and α in Eq. (27) are now fixed positive constants. For this purpose, we define the following function:

$$F(\Delta\phi, \lambda) \equiv \langle|\bar Z(\theta) + \lambda|^\alpha\rangle = \langle|Z(\theta + \Delta\phi) - Z(\theta) + \lambda|^\alpha\rangle. \tag{28}$$

On the other hand, using (26), the charge-balance constraint (5) becomes

$$\langle\text{sgn}[\bar Z(\theta) + \lambda]|\bar Z(\theta) + \lambda|^\beta\rangle = 0, \tag{29}$$

because $\frac{1}{2\pi}\langle f_{\text{opt},\,p}(\theta)\rangle = \frac{1}{2\pi}\|\bar Z(\theta) + \lambda\|_q^{-\beta}\langle\text{sgn}[\bar Z(\theta) + \lambda]|\bar Z(\theta) + \lambda|^\beta\rangle$, and $\|\bar Z(\theta) + \lambda\|_q$ is a non-zero constant. Therefore, similarly to (28), the following function is defined:

$$G(\Delta\phi, \lambda) \equiv \langle\text{sgn}[\bar Z(\theta) + \lambda]|\bar Z(\theta) + \lambda|^\beta\rangle. \tag{30}$$

Consequently, for maximizing $F(\Delta\phi, \lambda)$ under the constraint $G(\Delta\phi, \lambda) = 0$, the function

$$H(\Delta\phi, \lambda) \equiv F(\Delta\phi, \lambda) + \mu G(\Delta\phi, \lambda) \tag{31}$$

is naturally introduced, where μ is a Lagrange multiplier. The optimal solutions to Eq. (31) are obtained by Eqs. (53)–(55). One of the main theorems in this paper can now be stated as

follows:

Theorem 1. *For $1 < p < \infty$, suppose that $Z(\theta)$ satisfies the following assumptions* (i–iv)*:*

(i) *Z is twice differentiable (and hence, locally Lipschitz continuous).*

(ii) *$g(\theta) = \bar{Z}(\theta) + \lambda = 0$ given in Eq. (24) has (a finite number of) isolated zeros θ_*,*

(iii) *$H(\Delta\phi, \lambda)$ defined in Eq. (31) has a finite number of isolated optimal solutions $(\Delta\phi_*, \lambda_*)$, and*

(iv) *at each optimal solution of H, the bordered Hessian ([31]) $|\mathcal{H}(H)| \neq 0$, and $\bar{Z}'(\theta_*) \neq 0$ for each θ_* in* (ii).

Namely, assume that Z is smooth and generic in the above sense; then the global optimal forcing $f_{\mathrm{opt},p} \in L^p(S)$ is given by Eq. (26) if the 'best' solution $(\overline{\Delta\phi}_*, \bar{\lambda}_*)$ determined by Eqs. (53)–(55) exists; in this case, $F(\overline{\Delta\phi}_*, \bar{\lambda}_*)$ defined in Eq. (28) is the largest among all possible optima of $F(\Delta\phi_*, \lambda_*)$ under the constraint $G(\Delta\phi, \lambda) = 0$.

The proof of this theorem is given in Section 9.1. Now, it is natural to ask, besides the global optimal forcing, what sort of other local optimal forcings are possible for a given generic $Z(\theta)$? Answering requires the solutions $(\Delta\phi_*, \lambda_*)$ to Eqs. (53) and (54) to be characterized. Here we show that $(\Delta\phi, \lambda) = (0, 0)$ and $(\pm\pi, 0)$ are always solutions to Eqs. (53) and (54).

First, the solution $(0, 0)$ satisfies Eqs. (53) and (54), but this solution corresponds to $f_{\mathrm{opt},\,p}(\theta) \equiv 0$ and $\Gamma(\phi) \equiv 0$. Thus, the solution $(0, 0)$ corresponds to a trivial situation and so is hereafter discarded whenever it appears.

Next, the solutions $(\Delta\phi_*, \lambda_*) = (\pm\pi, 0)$ always exist, as shown below. Plugging $\Delta\phi = \pi$ and $\lambda = 0$ into Eq. (53) and letting $I \equiv \langle \mathrm{sgn}[Z(\theta+\pi) - Z(\theta)]|Z(\theta+\pi) - Z(\theta)|^\beta Z'(\theta+\pi)\rangle$, after changing θ to $\theta + \pi$, we obtain $I = -\langle \mathrm{sgn}[Z(\theta+\pi) - Z(\theta)]|Z(\theta+\pi) - Z(\theta)|^\beta Z'(\theta)\rangle$ since $Z(\theta)$ is a periodic function: $Z(\theta + 2\pi) = Z(\theta)$, and $Z'(\theta + 2\pi) = Z'(\theta)$. Summing the above two equations for I, we have $2I = \langle \mathrm{sgn}[Z(\theta+\pi) - Z(\theta)]|Z(\theta+\pi) - Z(\theta)|^\beta [Z(\theta+\pi) - Z(\theta)]'\rangle = \frac{1}{\beta+1} \cdot [|Z(\theta+\pi) - Z(\theta)|^{\beta+1}] = 0$. Thus, $I = 0$ is obtained for $(\pi, 0)$, and the solution $(\pi, 0)$ to Eq. (53) is verified. An analogous calculation verifies the solution $(-\pi, 0)$.

Finally, again plugging $\Delta\phi = \pm\pi$ and $\lambda = 0$ into Eq. (54) and letting $J \equiv \langle \mathrm{sgn}[Z(\theta \pm \pi) - Z(\theta)]|Z(\theta \pm \pi) - Z(\theta)|^\beta \rangle$ respectively for $\Delta\phi = \pm\pi$, if the same procedure is repeated, then $J = -\langle \mathrm{sgn}[Z(\theta+\pi) - Z(\theta)]|Z(\theta+\pi) - Z(\theta)|^\beta \rangle = -J$ is obtained. Thus, $J = 0$ and the solution $(\pm\pi, 0)$ to Eq. (54) is verified. ■

In addition to the solutions $(\pm\pi, 0)$, $Z(\theta)$ often allows other solutions which can be numerically identified, as shown in the example in Section 6.1.

5.2. Case of $p = \infty$

For $p = \infty$, from Lemma 4, the global optimal solution $f_{\mathrm{opt},\,\infty}$ is obtained by Eq. (18) and $g(\theta) = \bar{Z}(\theta) + \lambda$:

$$f_{\mathrm{opt},\,\infty}(\theta) = M\mathrm{sgn}[\bar{Z}(\theta) + \lambda], \tag{32}$$

which results in

$$\langle f_{\mathrm{opt},\,\infty}\, g\rangle = M\langle|\bar{Z}(\theta) + \lambda|\rangle. \tag{33}$$

Then, similarly to Eqs. (28), (30), and (31), the following functions,

$$\begin{aligned} F_\infty(\Delta\phi, \lambda) &\equiv \langle|\bar{Z}(\theta) + \lambda|\rangle, \\ G_\infty(\Delta\phi, \lambda) &\equiv \langle \mathrm{sgn}[\bar{Z}(\theta) + \lambda]\rangle, \\ H_\infty(\Delta\phi, \lambda) &\equiv F_\infty(\Delta\phi, \lambda) + \mu G_\infty(\Delta\phi, \lambda), \end{aligned} \tag{34}$$

are respectively defined for maximizing the locking range $(= \frac{M}{2\pi} F_\infty)$ under the charge-balance constraint ($G_\infty = 0$). Note that $G_\infty(\Delta\phi, \lambda) = 0$ is obtained from Eqs. (5) and (32), and $H_\infty(\Delta\phi, \lambda)$ is introduced for the same reason as Eq. (31). Thus, analogous to Theorem 1, the following theorem is obtained:

Theorem 2. *For $p = \infty$, suppose that $Z(\theta)$ satisfies the following assumptions* (i–iv)*:*

(i) *Z is twice differentiable,*

(ii) *$g(\theta) = \bar{Z}(\theta) + \lambda = 0$ has (a finite number of) isolated zeros θ_*,*

(iii) *$H_\infty(\Delta\phi, \lambda)$ in Eq. (34) has a finite number of isolated optimal solutions $(\Delta\phi_*, \lambda_*)$, and*

(iv) *at each optimal solution of H_∞, the bordered Hessian $|\mathcal{H}(H_\infty)| \neq 0$, and $\bar{Z}'(\theta_*) \neq 0$ for each θ_* in* (ii).

Namely, assume that Z is smooth and generic in the above sense; then the global optimal forcing $f_{\mathrm{opt},\,\infty} \in L^\infty(S)$ is given by Eq. (32) if the best solution $(\overline{\Delta\phi}_*, \bar{\lambda}_*)$ determined by Eqs. (69a)–(69c) exists.

As the proof is essentially the same as the one of Theorem 1, only the differences between them are addressed in Section 9.2. Note, similarly to the case of $1 < p < \infty$, the solutions $(\pm\pi, 0)$ exist, although this verification is omitted here, as it is identical to that in the case of $1 < p < \infty$. Other solutions to Eqs. (69a), (69b) are numerically identified as shown in Section 6.2.

5.3. Case of $p = 1$

For $p = 1$, from Lemma 5, the *ideal* locking range is given by $\frac{M}{2\pi}\|g\|_\infty$ as $\epsilon \to 0$. Here this is realized for a concrete example of $g(\theta) = \bar{Z}(\theta) + \lambda$ given in Eq. (24) as follows.

Theorem 3. *For $p = 1$, suppose that $Z(\theta)$ satisfies the following assumptions* (i), (ii), *and* (iii)*:*

(i) *Z is locally Lipschitz continuous,*

(ii) *$g(\theta) = \bar{Z}(\theta) + \lambda$ $(= Z(\theta + \Delta\phi) - Z(\theta) + \lambda)$ achieves the maximum and the minimum, respectively at some $\theta = \theta_{\max}$ and $\theta = \theta_{\min}$, and*

(iii) *the maximum of $\bar{Z}(\theta)$ −* the minimum *of $\bar{Z}(\theta)$ $(= \bar{Z}(\theta_{\max}) - \bar{Z}(\theta_{\min}))$ is maximized for a particular value of $\Delta\phi = \Delta\phi_{\max}$ and this choice of $\Delta\phi_{\max}$ (and its associated $\theta_{\max}$, $\theta_{\min}$) is unique for a given Z.*

Namely, assume that Z is continuous and generic in the above sense; then the pair of two pulses

$$f_{*,\,1}(\theta) = -M[\Delta(\theta + \Delta\phi_{\max}) - \Delta(\theta)] \tag{35}$$

realizes the ideal *locking range $\frac{M}{2\pi}\|g\|_\infty$ (obtained in Lemma 5) as $\epsilon \to +0$ (in Eq. (22)), where $\Delta\phi_{\max}$ satisfies $\Delta\phi_{\max} = \theta_{\max} - \theta_{\min}$.*

The proof of this theorem is given in Section 9.3. We note that, in practical situations, the above $\Delta\phi_{\max}$ is numerically determined for any given Z, as shown in the example of Section 6.3.

5.4. Case of m:n entrainment

In the analysis starting from Eq. (23a), we have implicitly assumed 1:1 entrainment. Now we consider what happens for general m:n entrainment. As mentioned in Section 3, if $m \neq n$, neither the non-trivial *ideal* solution given by Eq. (26) for $1 < p < \infty$ nor the one given by Eq. (32) for $p = \infty$ is realized. However, for the case of m:1 entrainment, an 'asymptotically *ideal*' forcing (*i.e.*, a forcing asymptotically realizing the *ideal* locking range) is constructed as follows.

Fig. 3 illustrates how an asymptotically *ideal* forcing is constructed by starting from m copies with the *ideal* forcing with prime period T_0 for 1:1 entrainment and adding a certain small perturbation such that the m copies of the forcing become a single forcing with prime period mT_0 while still satisfying the constraints (4) and (5). Thus, the resulting locking range becomes arbitrarily close to the *ideal* one (which is realized only in 1:1 entrainment) as the perturbation becomes smaller, since the associated $\Gamma_{m/1}$ in Eq. (3) becomes arbitrarily close to the $\Gamma_{1/1}$ of the best forcing for 1:1 entrainment.

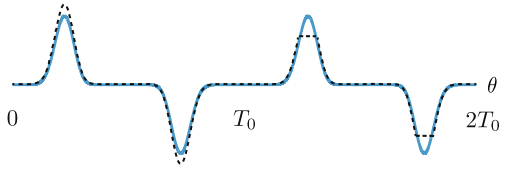

Fig. 3. Schematic illustrations of forcing waveforms for m:1 entrainment (*e.g.*, $m = 2$). The solid blue line shows the m (=2) copies of the *ideal* forcing f in Eq. (26) with prime period T_0. The dotted black line shows a slightly perturbed forcing, constructed from the m copies of the *ideal* forcing, with prime period $2T_0$.

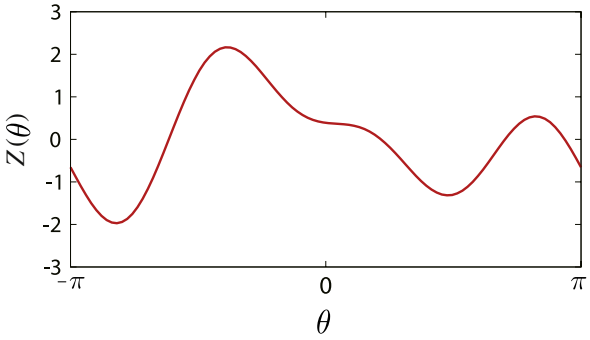

Fig. 4. Graph of $Z(\theta)$ in (36).

In addition, Lemmata 1 and 2 imply that it is not rewarding to search for any other '*ideal*' forcings for m:n entrainment besides Eq. (26), since the *ideal* forcing is uniquely given by Eq. (26) for any $m \neq n$ (Lemma 1) and actually does not exist except for the trivial zero forcing (Lemma 2). Thus, the above argument proves the following:

Theorem 4. *Assume m and n are positive relatively prime integers and $m \neq n$. For $1 < p < \infty$, suppose that $Z(\theta)$ satisfies the assumptions in Theorem 1, and for $p = \infty$, suppose that $Z(\theta)$ satisfies the assumptions in Theorem 2. Then the* ideal *forcing (26) for $1 < p < \infty$ does not exist for the general m: n entrainment (in $L^p(S)$), and neither does the* ideal *forcing (32) for $p = \infty$ (in $L^\infty(S)$). However, if $n = 1$, an 'asymptotically* ideal*' forcing is constructed for $1 < p < \infty$ (or $p = \infty$) from m copies of the forcing (26) (or (32)) plus some arbitrary small perturbation such that both constraints (4) and (5) are satisfied (as illustrated in Fig. 3).*

6. Numerical verification of optimal forcing waveforms

Here some concrete examples of Z are considered to numerically verify the theoretical results in Section 5. For this purpose, first, a randomly generated $Z(\theta)$ as shown in Fig. 4 is chosen, which includes some higher harmonics, as usually observed in chemical or circadian oscillators:

$$\begin{aligned} Z(\theta) = {} & 0.745705\cos\theta - 0.666276\sin\theta - 0.134064\cos 2\theta \\ & - 0.940493\sin 2\theta - 0.222622\cos 3\theta \\ & + 0.768401\sin 3\theta. \end{aligned} \tag{36}$$

For this particular $Z(\theta)$, a systematic numerical study is carried out to identify the optimal solutions of $J[f]$, as shown in Sections 6.1–6.3 below. In addition to the example of (36), the weakly stimulated Hodgkin–Huxley neuron model, whose phase response function is given in [17,28], is also considered:

$$\begin{aligned} Z(\theta) = {} & 0.176116 + 0.371736\cos\theta - 0.740283\sin\theta \\ & - 0.819478\cos 2\theta + 0.00225226\sin 2\theta \\ & + 0.181875\cos 3\theta + 0.403816\sin 3\theta \\ & + 0.111446\cos 4\theta - 0.0892503\sin 4\theta \\ & - 0.0127103\cos 5\theta - 0.0165083\sin 5\theta. \end{aligned} \tag{37}$$

As the procedure for obtaining all (local and global) optimal forcings is the same for both examples (36) and (37), we explain the case of (36) in detail, and for the case of (37), we omit detailed numerical data here and just mention the numerical results.

6.1. Case of $1 < p < \infty$ for the example of (36)

For the example of (36), here we numerically identify the optimal forcings for the case of $1 < p < \infty$, as follows. The case of $p = \infty$ and the case of $p = 1$ are respectively considered in Sections 6.2 and 6.3.

To determine the parameter pair $(\Delta\phi, \lambda)$ of $f_{\mathrm{opt},\,p}(\theta)$ in Eq. (26), we have numerically solved Eqs. (53) and (54) for $(\Delta\phi, \lambda)$, and checked if the obtained $(\Delta\phi, \lambda)$ satisfies Eq. (55); the results are listed in Table 1. But, first, to capture the global features of Eqs. (53) and (54), we begin by plotting the solution curves of $(\Delta\phi, \lambda)$ for Eqs. (53) and (54), respectively, in order to locate all crossing points along these solution curves. These are shown in Fig. 5 for the cases of $p = 1.01, 1.1, 2, 5$, and 10. In addition, Fig. 6 shows a magnification of Fig. 5 around each crossing point for the case of $p = 1.01$. Having located all crossing points, we can determine their position as precisely as possible by using the Newton–Raphson method, as below. The above steps constitute an algorithm for obtaining the optimal forcing for $1 < p < \infty$.

Although these solution curves look a bit complicated, some information about them can be obtained analytically, as follows. For Eqs. (53) and (54), respectively, let $\langle \mathrm{sgn}[\bar{Z}(\theta) + \lambda]|\bar{Z}(\theta) + \lambda|^\beta Z'(\theta + \Delta\phi)\rangle \equiv S_p(\Delta\phi, \lambda)$ and $\langle \mathrm{sgn}[\bar{Z}(\theta) + \lambda]|\bar{Z}(\theta) + \lambda|^\beta\rangle \equiv T_p(\Delta\phi, \lambda)$ (=$G(\Delta\phi, \lambda)$ in Eq. (30)). Then, it is clear that $T_p(\Delta\phi, \lambda)$ is a C^1 function, since both partial derivatives of $T_p(\Delta\phi, \lambda)$ exist, as shown in Eqs. (48) and (49), and are continuous, as proved in Appendix F. Moreover, $\frac{\partial T_p(\Delta\phi,\lambda)}{\partial\lambda} = \beta\langle|\bar{Z}(\theta) + \lambda|^{\beta-1}\rangle > 0$ for any $\Delta\phi$ from Eq. (51f). Thus, by the implicit function theorem, a C^1 function $\lambda(\Delta\phi)$ satisfying $T_p(\Delta\phi, \lambda(\Delta\phi)) = 0$ is defined in the neighborhood of every $\Delta\phi_*$ satisfying $T_p(\Delta\phi_*, \lambda(\Delta\phi_*)) = 0$. In addition, this $\lambda(\Delta\phi)$ is single-valued, since $\frac{\partial T_p(\Delta\phi,\lambda)}{\partial\lambda} > 0$ and $T_p(\Delta\phi, \lambda) \to \pm\infty (\lambda \to \pm\infty)$ for any $\Delta\phi$. Therefore, the solution curve $T_p = 0$ for Eq. (54) is obtained as a C^1, single-valued function $\lambda(\Delta\phi)$ over $S = [-\pi, \pi]$, as observed in Fig. 5. ■

On the other hand, in $S_p(\lambda, \Delta\phi) = \langle \mathrm{sgn}[\bar{Z}(\theta) + \lambda]|\bar{Z}(\theta) + \lambda|^\beta Z'(\theta + \Delta\phi)\rangle$, the term $\mathrm{sgn}[\bar{Z}(\theta) + \lambda]|\bar{Z}(\theta) + \lambda|^\beta \to \pm\infty (\lambda \to \pm\infty)$. However, $S_p(\lambda, \Delta\phi)$ does not necessarily go to $\pm\infty$ as λ goes to $\pm\infty$, since the above term is weighted by $Z'(\theta + \Delta\phi)$. Thus, depending on the value of $\Delta\phi$, $S_p(\lambda, \Delta\phi) = 0$ might have no solution for λ. In addition, the solution curve $S_p = 0$ can be complicated, as observed in Fig. 5.

Next, we solve Eqs. (53) and (54) using the Newton–Raphson method. The Jacobi matrices for Eqs. (53) and (54) are obtained from Eq. (51) and the initial values of the iteration are chosen from the numerically obtained crossing points of $S_p = 0$ and $T_p = 0$ mentioned above. The obtained results for $p = 1.01, 1.1, 2, 5$, and 10 are listed in Table 1. In Table 1(a), the seven obtained solutions for $p = 1.01$ are listed. There being seven solutions implies that the total number of solutions is $7\times2+1-1 = 14$, since there is an extra trivial solution $(0, 0)$ corresponding to the '+1' in '$7\times2+1-1$', two solutions $(\pm\pi, 0)$ are identified, corresponding to the '-1', and as mentioned in Section 9.1.2, a symmetry $(\Delta\phi, \lambda) \leftrightarrow (-\Delta\phi, -\lambda)$ exists, which corresponds to the '$\times2$'. Note that this kind of argument regarding the total number of solutions is not possible in the Euler–Lagrange formalism due to its locality in its mathematical nature, and there is no guarantee of finding all possible solutions (in a rigorous sense).

For each of the seven solutions shown in Fig. 5(a) and Fig. 6, the locking range is obtained from Eq. (27) by setting $M = 1$ and

Table 1
Solutions $(\Delta\phi, \lambda)$ to Eqs. (53) and (54), their associated locking ranges, and $|\mathcal{H}(H)|$: (a) $p = 1.01$, (b) $p = 1.1$, (c) $p = 2$, (d) $p = 5$, and (e) $p = 10$. Here 'theory' and 'GA' respectively indicate the results from theoretical prediction and a direct GA search.

(a) $p = 1.01$
solutions 1: $(\Delta\phi, \lambda) = (-3.1415927, 0.0000000)$, locking range (theory) = 3.0235540, locking range (GA) = 3.0234959, $|\mathcal{H}(H)| = 4.9714938 \times 10^{149}$ (>0)
solutions 2: $(\Delta\phi, \lambda) = (-2.7635739, -0.5681094)$, locking range (theory) = 2.8134444, $|\mathcal{H}(H)| = -8.1140349 \times 10^{140}$ (<0)
solutions 3: $(\Delta\phi, \lambda) = (-2.6739647, -0.5640646)$, locking range (theory) = 2.8185146, locking range (GA) = not found, $|\mathcal{H}(H)| = 1.6695215 \times 10^{140}$ (>0)
solutions 4: $(\Delta\phi, \lambda) = (-2.4248451, -0.4290781)$, locking range (theory) = 2.8022469, $|\mathcal{H}(H)| = -3.2519168 \times 10^{139}$ (<0)
solutions 5: $(\Delta\phi, \lambda) = (-1.9047696, 0.5266019)$, locking range (theory) = 2.8935164, locking range (GA) = 2.8933493, $|\mathcal{H}(H)| = 4.0131891 \times 10^{143}$ (>0)
solutions 6: $(\Delta\phi, \lambda) = (-1.6467727, 0.9915109)$, locking range (theory) = 2.8644525, $|\mathcal{H}(H)| = -1.5284447 \times 10^{143}$ (<0)
solutions 7: $(\Delta\phi, \lambda) = (-1.2455892, 0.8126150)$, locking range (theory) = 3.1775924, locking range (GA) = 3.1771833, $|\mathcal{H}(H)| = 1.8067790 \times 10^{156}$ (>0)

(b) $p = 1.1$
solutions 1: $(\Delta\phi, \lambda) = (-3.1415927, 0.0000000)$, locking range (theory) = 2.5532186, locking range (GA) = 2.5501987, $|\mathcal{H}(H)| = 3.5228057 \times 10^{14}$ (>0)
solutions 2: $(\Delta\phi, \lambda) = (-2.5402401, -0.4637718)$, locking range (theory) = 2.4093452, $|\mathcal{H}(H)| = -3.6750468 \times 10^{13}$ (<0)
solutions 3: $(\Delta\phi, \lambda) = (-1.2720412, 0.7924492)$, locking range (theory) = 2.6747648, locking range (GA) = 2.6622400, $|\mathcal{H}(H)| = 1.9969242 \times 10^{15}$ (>0)

(c) $p = 2$
solutions 1: $(\Delta\phi, \lambda) = (-3.1415927, 0.0000000)$, locking range (theory) = 1.8110770, locking range (GA) = 1.8110770, $|\mathcal{H}(H)| = 3.1500000$ (>0)
solutions 2: $(\Delta\phi, \lambda) = (-2.2828510, 0.0000000)$, locking range (theory) = 1.6695480, $|\mathcal{H}(H)| = -3.6826624$ (<0)
solutions 3: $(\Delta\phi, \lambda) = (-1.3864149, 0.0000000)$, locking range (theory) = 1.8807507, locking range (GA) = 1.8807341, $|\mathcal{H}(H)| = 6.2100798$ (>0)

(d) $p = 5$
solutions 1: $(\Delta\phi, \lambda) = (-3.1415927, 0.0000000)$, locking range (theory) = 1.6404898, locking range (GA) = 1.6412232, $|\mathcal{H}(H)| = 0.1105319$ (>0)
solutions 2: $(\Delta\phi, \lambda) = (-2.2037685, -0.0579161)$, locking range (theory) = 1.4257440, $|\mathcal{H}(H)| = -1.4058183$ (<0)
solutions 3: $(\Delta\phi, \lambda) = (-1.4058325, -0.4169387)$, locking range (theory) = 1.6581230, locking range (GA) = 1.6550836, $|\mathcal{H}(H)| = 0.3035783$ (>0)

(e) $p = 10$
solutions 1: $(\Delta\phi, \lambda) = (-3.1415927, 0.0000000)$, locking range (theory) = 1.6035454, locking range (GA) = 1.6048877, $|\mathcal{H}(H)| = 0.0366672$ (>0)
solutions 2: $(\Delta\phi, \lambda) = (-2.1974857, -0.0725039)$, locking range (theory) = 1.3690487, $|\mathcal{H}(H)| = -1.4298989$ (<0)
solutions 3: $(\Delta\phi, \lambda) = (-1.4225536, -0.5477614)$, locking range (theory) = 1.6052778, locking range (GA) = 1.6032058, $|\mathcal{H}(H)| = 0.3040965$ (>0)

$|\mathcal{H}(H)|$ is evaluated, as shown in Table 1(a). From these results, the following facts are now clarified.

(i) The global optimal solutions are $(\Delta\phi, \lambda) \sim (-1.245, 0.812)$ (solution 7) and its symmetric counterpart $(1.245, -0.812)$.

(ii) Solutions 1, 3, and 5 are all local optimal, since $|\mathcal{H}(H)| > 0$. In contrast, solutions 2, 4, and 6 are not, since $|\mathcal{H}(H)| < 0$ [31].

Figs. 7(a)–(f) show $R(\Delta\phi)$ along the solution curve T_p parameterized by $\Delta\phi$, which clearly characterizes the optimality of solutions and their associated locking ranges for $p = 1.01$, 1.1, 2, 5, 10, and ∞, respectively. Since $R(\Delta\phi)$ is an even function, we plot only the half for $\Delta\phi \in [-\pi, 0]$. As we see in Fig. 7(a), optimality of $R(\Delta\phi)$ for each solution is consistent with facts (i) and (ii) above.

To check the above numerical results, we also perform a brute force search of optimal forcings with a genetic algorithm (GA) directly for Eq. (2) under the constraints of (4) and (5) with $M = 1$. In doing so, we discretize the forcing f with sufficiently small mesh sizes, as shown by $f_{\text{opt}}(\theta)_{\text{GA}}$ in Figs. 8–12, where a perfect match is observed between the theoretical predictions (the above numerical results) and the direct GA search.

Returning to the case of $p = 1.01$ discussed previously, as shown in Fig. 8, the locally optimal solutions 1, 5, and 7 are captured by the GA search, but the non-optimal solutions 2, 4, and 6 are not. Also, for a technical reason, our GA search is not able to capture the locally optimal solution 3. The reason can be understood as follows. By plotting the $\Gamma(\phi)$ associated with this solution 3 (Fig. 13), we can see that the locking range R for this particular solution 3 ($\Delta\phi \sim -2.6739$) is suboptimal, since there is one other potentially optimal $\bar{R}$, which gives the actual best R of this $\Gamma(\phi)$, although solution 3 is locally optimal in the two-parameter space $(\Delta\phi, \lambda)$. The problem arises because our GA algorithm always evaluates only the best $\bar{R}$ during its search, and so solution 3, like non-optimal solutions 2, 4, and 6, are ignored; therefore, solution 3 does not appear in Fig. 8(b).

6.2. Case of $p = \infty$ for the example of (36)

Similarly to the case of $1 < p < \infty$, Eqs. (69a) and (69b) are solved for $(\Delta\phi, \lambda)$ to determine $f_{\text{opt},\,\infty}(\theta)$ in (32). Again we begin by plotting the solution curves of $(\Delta\phi, \lambda)$ for Eqs. (69a) and (69b), which are shown in Fig. 14. Having located all crossing points, their precise positions are determined with the Newton–Raphson method. The above steps constitute an algorithm for determining $f_{\text{opt},\,\infty}$.

Notice that, in the shaded regions, $\langle \text{sgn}[\bar{Z}(\theta)+\lambda]Z'(\theta+\Delta\phi)\rangle \equiv 0$ holds since $\bar{Z}(\theta) + \lambda$ becomes always positive (or negative) and therefore $\langle \text{sgn}[\bar{Z}(\theta) + \lambda]Z'(\theta + \Delta\phi)\rangle = \langle Z'(\theta + \Delta\phi)\rangle = 0$ (or $-\langle Z'(\theta + \Delta\phi)\rangle = 0$). In this case, $p = \infty$, the total number of the solutions is $3 \times 2 + 1 - 1 = 6$, which includes the trivial solution $(0, 0)$. Precise values of the solutions to Eqs. (69a) and (69b) are obtained by the Newton–Raphson method, in which the Jacobi matrices of Eqs. (69a) and (69b) are given by Eq. (68). The results are listed in Table 2, in which we observe a perfect match between the theoretical results from Eq. (32) and the GA search results, which is also seen in Fig. 15.

6.3. Case of $p = 1$ for the example of (36)

First, for the case of $p = 1$, the two optimal parameters $\Delta\phi$ and λ are given by $\Delta\phi = \Delta\phi_{\max}$ and $\lambda = -\frac{1}{2}[\bar{Z}(\theta_{\max}) + \bar{Z}(\theta_{\min})]$, respectively, from the argument in Section 5.3 and from Eq. (74) in Section 9.3. This $\Delta\phi_{\max}$ is numerically obtained as follows: We plot the graph $\Gamma_0(\phi) = M[Z(\phi + \Delta\phi) - Z(\phi)]$ for a given $\Delta\phi \in [-\pi, 0]$, and then gradually vary this parameter, again plotting the graph of $\Gamma_0(\phi)$ for each value. Thus, the locking range $R =$ (the maximum of Γ_0) − (the minimum of Γ_0) is obtained as a function of $\Delta\phi$, as shown in Fig. 16a. Note that $R(\Delta\phi)$ is an even function, due to the symmetry of the forcing (35), and so we plot only half of it in Fig. 16a. Also, λ is determined once $\Delta\phi_{\max}$ is obtained; $\Delta\phi_{\max}$ determines $\theta_{\max}$ and $\theta_{\min}$ from the graph of Γ_0, which is described in Section 9.3. The above steps constitute an algorithm for obtaining $\Delta\phi_{\max}$ and λ, which results in the global optimal forcing $f_{\text{opt},\,1}$. As shown in Fig. 16a, the resulting graph $R(\Delta\phi)$ for $p = 1$ is indistinguishable from the graph of $R(\Delta\phi)$ for $p = 1.01$ in Fig. 7(a), which shows that the best $\Delta\phi$ is around -1.245 and the second best $\Delta\phi$ is $-\pi$. We also note this value of optimal $\Delta\phi \sim -1.245$ is close to, but slightly different from, the phase difference between the maximum and minimum of $Z(\theta)$, which is about -1.3660, as measured in Fig. 4.

Next, we verify the above predictions about the best impulsive forcing through systematic numerical simulations as follows. First,

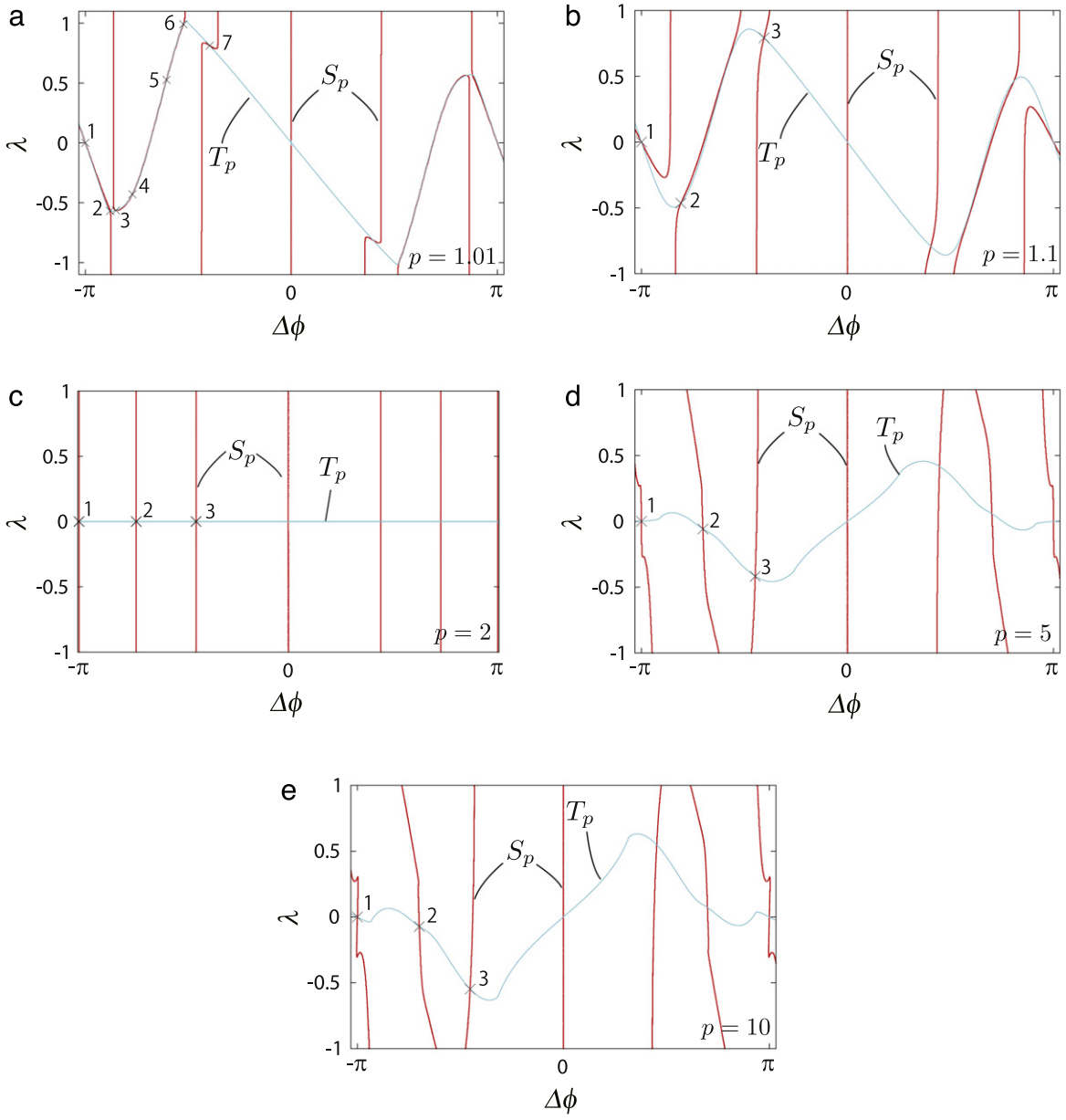

Fig. 5. Solution curves S_p for Eq. (53) and solution curve T_p for Eq. (54): (a) $p = 1.01$, (b) $p = 1.1$, (c) $p = 2$, (d) $p = 5$, and (e) $p = 10$.

Table 2
Solutions $(\Delta\phi, \lambda)$ to Eqs. (69a) and (69b), their locking ranges, and $|\mathcal{H}(H)|(p = \infty)$.

solutions 1: $(\Delta\phi, \lambda) = (-3.1415927, 0.0000000)$, locking range (theory) $= 1.5726076$, locking range (GA) $= 1.5708262$, $\lvert\mathcal{H}(H)\rvert = 0.0097912$ (>0)
solutions 2: $(\Delta\phi, \lambda) = (-2.1941055, -0.0833533)$, locking range (theory) $= 1.3214593$, $\lvert\mathcal{H}(H)\rvert = -1.3194747$ (<0)
solutions 3: $(\Delta\phi, \lambda) = (-1.4456283, -0.6738817)$, locking range (theory) $= 1.5585141$, locking range (GA) $= 1.5617386$, $\lvert\mathcal{H}(H)\rvert = 0.0995980$ (>0)

we check if this $R(\Delta\phi)$ for $p = 1$ is consistent with the locking range directly obtained from the phase model (2) with $\Gamma_0(\phi)$ in (77). The results are plotted as +s in Fig. 16b and show perfect agreement with the theoretical prediction. Similarly, the results from Eq. (1) with the weak impulses of (75) (width $= 0.07$, amplitude $= 1.14$) exhibit a perfect match with the theory, as shown by the ×s in Fig. 16b. In addition, Fig. 17 shows the Arnold tongues for five different impulsive forcings (35) with $\Delta\phi_{\max}$ being set to $-\pi$, -2.12058, -1.72788, -1.24470, and -0.62832. Notice that we include non-optimal values, in order to compare locking ranges. Numerical simulations of Eq. (1) are carefully carried out by using the 4th-order Runge–Kutta method with a timestep of 0.001. The result shows the predicted best impulsive forcing is indeed the best among these five forcings.

6.4. Case of the Hodgkin–Huxley neuron model (37)

Repeating the same procedure as in Sections 6.1–6.3, we obtain all the optimal forcings for the Hodgkin–Huxley neuron model in (37) as follows. For the cases of $1 < p < \infty$ and $p = \infty$, the parameter pairs $(\Delta\phi, \lambda)$ in $f_{\text{opt},p}(\theta)$ are obtained as listed in Table 3. These results show that for the example of (37) the number of optimal forcings is always less than that of the previous example, (36). This seems to reflect the fact that Eq. (37) has weaker higher harmonics than those in Eq. (36), making the solution curves S_p and T_p relatively simple.

Finally, for the case of $p = 1$, $\Delta\phi_{\max}$ is numerically obtained as $\Delta\phi_{\max} \sim -1.36094$ by the same procedure as in Section 6.3. Note

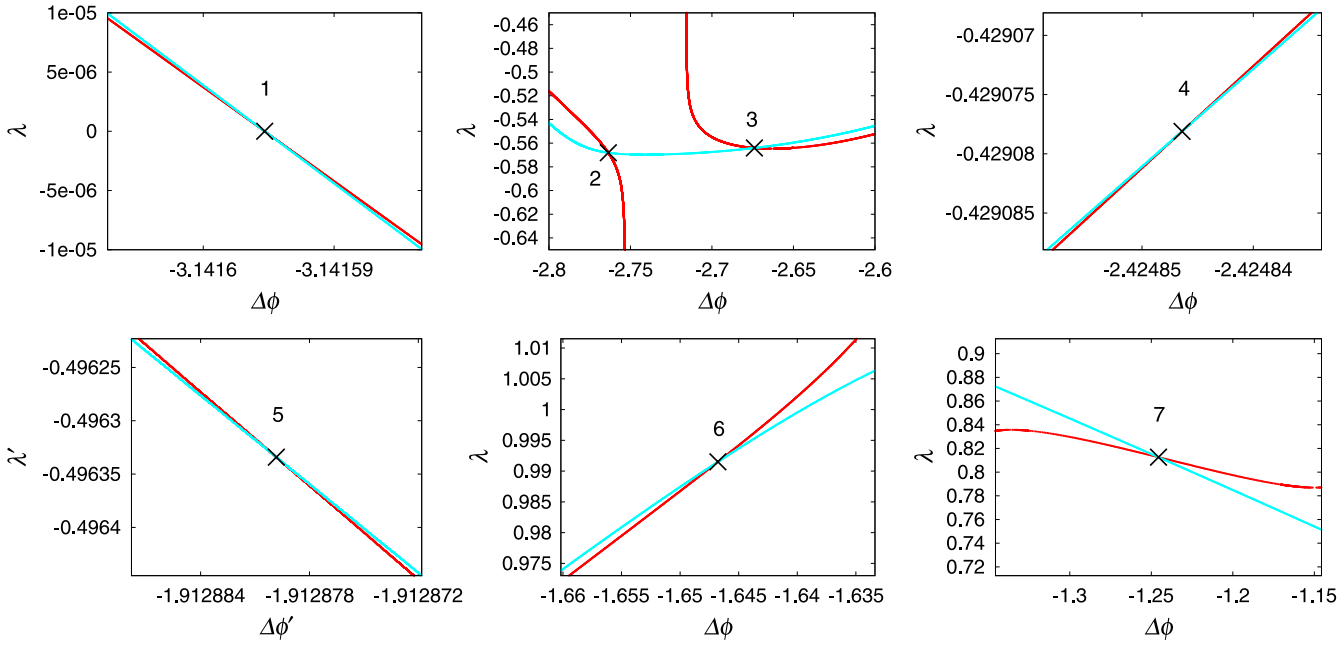

Fig. 6. Magnified solution curves of Eqs. (53) and (54) in the neighborhood of each crossing point ($p = 1.01$). For better resolution, a new coordinate ($\Delta\phi'$, λ') is introduced in the graph for solution 5: $\Delta\phi' = \cos\frac{\pi}{6}\cdot\Delta\phi - \sin\frac{\pi}{6}\cdot\lambda$ and $\lambda' = \sin\frac{\pi}{6}\cdot\Delta\phi + \cos\frac{\pi}{6}\cdot\lambda$.

Table 3
Solutions $(\Delta\phi, \lambda)$ to Eqs. (53) and (54), their associated locking ranges, and $|\mathcal{H}(H)|$: (a) $p = 1.01$, (b) $p = 1.1$, (c) $p = 2$, (d) $p = 5$, (e) $p = 10$, and (f) $p = \infty$. Here 'theory' and 'GA' respectively indicate the results from theoretical prediction and a direct GA search.

(a) $p = 1.01$
solutions 1: $(\Delta\phi, \lambda) = (-3.1415927, 0.0000000)$, locking range (theory) $= 2.2585700$, $\lvert\mathcal{H}(H)\rvert = -6.4861331 \times 10^{110}$ (<0)
solutions 2: $(\Delta\phi, \lambda) = (-1.3649363, 0.57040837)$, locking range (theory) $= 2.7613265$, locking range (GA) $= 2.7609771$, $\lvert\mathcal{H}(H)\rvert = 5.7290424 \times 10^{137}$ (>0)
(b) $p = 1.1$
solutions 1: $(\Delta\phi, \lambda) = (-3.1415927, 0.0000000)$, locking range (theory) $= 1.9165986$, $\lvert\mathcal{H}(H)\rvert = -1.2376531 \times 10^{10}$ (<0)
solutions 2: $(\Delta\phi, \lambda) = (-1.3980649, 0.54721054)$, locking range (theory) $= 2.3342603$, locking range (GA) $= 2.3338741$, $\lvert\mathcal{H}(H)\rvert = 2.1545556 \times 10^{13}$ (>0)
(c) $p = 2$
solutions 1: $(\Delta\phi, \lambda) = (-3.1415927, 0.0000000)$, locking range (theory) $= 1.3287487$, $\lvert\mathcal{H}(H)\rvert = -0.54999893$ (<0)
solutions 2: $(\Delta\phi, \lambda) = (-1.6150653, 0.0000000)$, locking range (theory) $= 1.4926698$, locking range (GA) $= 1.4925093$, $\lvert\mathcal{H}(H)\rvert = 2.153595723$ (>0)
(d) $p = 5$
solutions 1: $(\Delta\phi, \lambda) = (-3.1415927, 0.0000000)$, locking range (theory) $= 1.21853096$, locking range (GA) $= 1.2177683$, $\lvert\mathcal{H}(H)\rvert = 0.017074170$ (>0)
solutions 2: $(\Delta\phi, \lambda) = (-2.5085617, -0.23864305)$, locking range (theory) $= 1.209864499$, $\lvert\mathcal{H}(H)\rvert = -0.080256775$ (<0)
solutions 3: $(\Delta\phi, \lambda) = (-1.948572843, -0.23837645)$, locking range (theory) $= 1.2161630$, locking range (GA) $= 1.2162259$, $\lvert\mathcal{H}(H)\rvert = 0.18880119$ (>0)
(e) $p = 10$
solutions 1: $(\Delta\phi, \lambda) = (-3.1415927, 0.0000000)$, locking range (theory) $= 1.1965111$, locking range (GA) $= 1.1952760$, $\lvert\mathcal{H}(H)\rvert = 0.02247527398$ (>0)
(f) $p = \infty$
solutions 1: $(\Delta\phi, \lambda) = (-3.1415927, 0.0000000)$, locking range (theory) $= 1.1784578$, locking range (GA) $= 1.1783933$, $\lvert\mathcal{H}(H)\rvert = 0.012231488$ (>0)

that this value of $\Delta\phi_{\max}$ is consistent with the optimal solution of $\Delta\phi \sim -1.364$ for $p = 1.01$ in Table 3. An overview of the resulting optimal forcings is presented in Fig. 18.

7. Conclusions and discussion

First, we will summarize the previous sections, and then we will consider some extensions and possible applications of our results. One of the important results in this paper is the fact that the optimization problem posed in Section 1 can be solved using the equality condition of Hölder's inequality, which results in, for 1:1 entrainment, (i) a construction of the global optimal forcing in $L^p(S)$ (Theorem 1 for $1 < p < \infty$, and Theorem 2 for $p = \infty$), and (ii) a construction of pulse-like forcings in $L^1(S)$ by which the *ideal* locking range is asymptotically realized (Theorem 3 for $p = 1$; note that the uniqueness of such forcings is not proved here), and for m:n entrainment, and (iii) a proof of the non-existence of the *ideal* forcing and a characterization of an asymptotically *ideal* forcing for m:1 entrainment in $L^p(S)$ (Theorem 4). (iv) In addition to these, we establish definite algorithms (Sections 6.1 and 6.2) for obtaining the global optimal forcing for $1 < p \leq \infty$ and pulse-like forcings for $p = 1$. The numerical results in Section 6 verify the perfect match between the theory and independent, systematic numerical simulations.

On the other hand, some parts of our results can also be derived by using the Euler–Lagrange equation, and some useful components are included in the present study (*e.g.*, Eqs. (51) and (68) in Section 9) for their derivations. It seems rather natural that such direct connections should emerge between Hölder's inequality and the calculus of variation. In fact, such connections are historically known [32]. However, it is still worth investigating the application limits in our inequality approach to more general optimization problems. Also, from a practical point of view, it is important to clarify what sort of entrainment problems can be solved with inequalities. Further work along this line will be reported elsewhere.

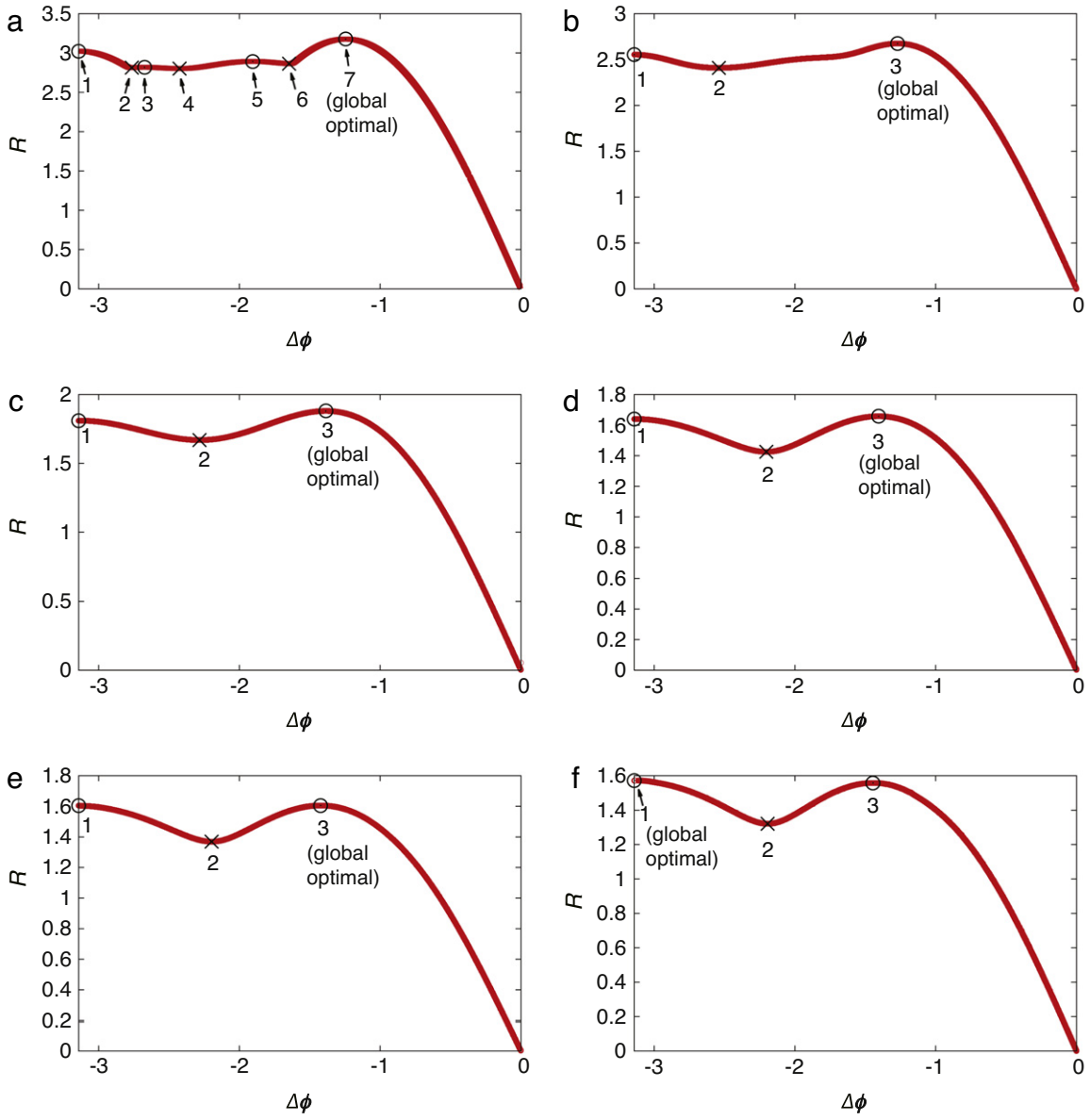

Fig. 7. $R(\Delta\phi)$ on T_p: (a) $p = 1.01$, (b) $p = 1.1$, (c) $p = 2$, (d) $p = 5$, (e) $p = 10$, and (f) $p = \infty$. In each graph, ∘ and × indicate the optimal and non-optimal solutions, respectively.

As mentioned in Section 1, the results in this paper constitute a useful design methodology for investigating entrainment issues in biology and neurophysiology, as well as electrical engineering; here, we briefly review some examples. (i) Zhai and Kiss have observed in an electro-chemical experiment that all the optimal forcings in our theory ($p = 1, 2, \infty$) actually optimize their locking ranges [33]. (ii) Sekiya, Nakada, and the author (H.T.) designed an injection-locking circuitry including CMOS (complementary metal–oxide semiconductor) ring oscillators [7] in microelectronics and class-E oscillators in power electronics, and verified that the theoretically obtained optimal forcing ($p = 1, 2$) optimized their locking ranges through systematic circuit simulations. In addition, (iii) Tsubo and H.T. have found our theoretical results useful also for optimizing entrainability in noisy oscillators in relation to neural activity, which will be reported elsewhere.

Finally, we point out some possible applications and extensions of our theory that we believe are interesting and may possibly be practically important. (i) Application to coupled oscillators (or excitable elements): For instance, our theory is immediately applicable if collective phase sensitivity [34–36] is obtained in such systems, where the whole system is effectively regarded as kind of a giant limit-cycle oscillator in high- (or infinite-) dimensional phase space. It should be noted that [37,38] are useful for obtaining such collective phase sensitivity in various situations. (ii) Optimization of the entrainment stability: This problem was first solved by using the Euler–Lagrange equation for the $p = 2$ case [17]. In contrast, if our theory is applied, then this problem can be solved (as we observe in this paper) under more general conditions simply by replacing $\bar{Z}(\theta)$ with $-Z'(\theta)$, similarly to [17]. (iii) Optimization of synchronization to common noise: [39,40] provide frameworks for optimizing the phase response function $Z(\theta)$ of the oscillator under certain common noises, in relation to [41]. Such frameworks for optimizing Z could be generalized and analyzed with the aid of the results in this paper, since optimization of the forcing f and that of Z are now equivalent by permuting Z and f if $\langle Zf \rangle$ is maximized. Also, needless to say, this idea of optimizing Z (for a given f) is now feasible for the noiseless situation considered in this paper. (iv) Controlling traveling pulses or waves in reaction–diffusion systems: [42] derives the associated phase sensitivity function, and the dynamics of traveling pulses

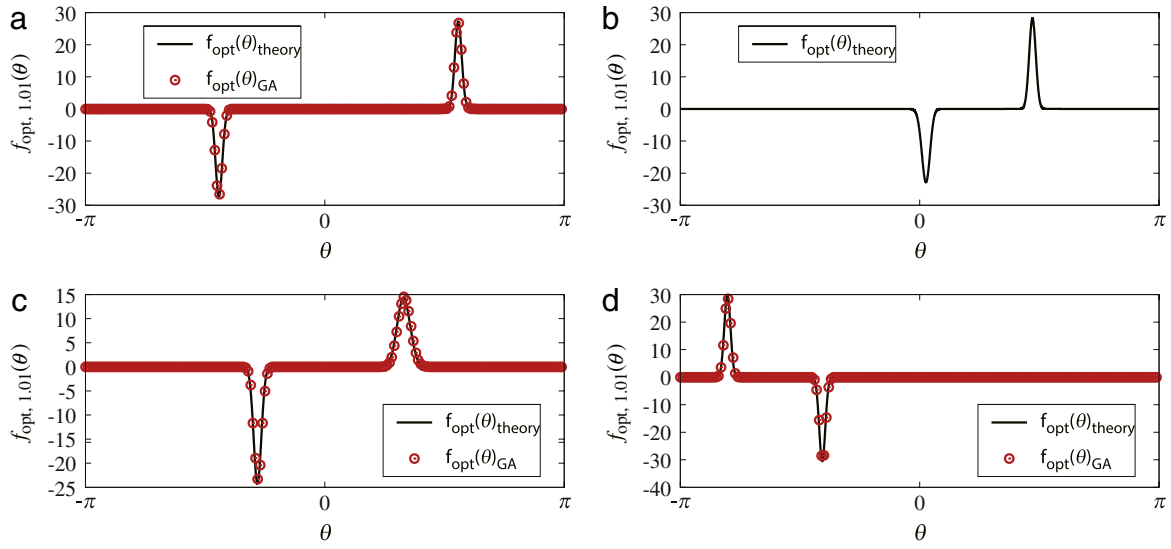

Fig. 8. Optimal forcing waveforms ($p = 1.01$): (a) $(\Delta\phi, \lambda) = (-\pi, 0)$, (b) $(\Delta\phi, \lambda) = (-2.6739647, -0.5640646)$, (c) $(\Delta\phi, \lambda) = (-1.9047696, 0.5266019)$, and (d) $(\Delta\phi, \lambda) = (-1.2455892, 0.8126150)$. Here $f_{\mathrm{opt}}(\theta)_{\mathrm{theory}}$ and $f_{\mathrm{opt}}(\theta)_{\mathrm{GA}}$ respectively indicate the results from the theoretical prediction (26) and a direct GA search.

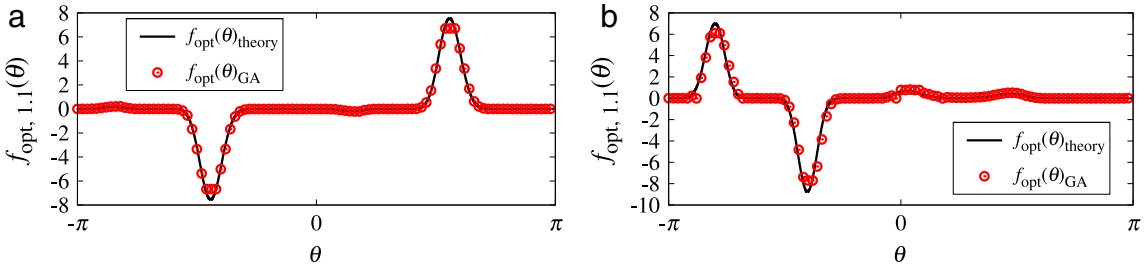

Fig. 9. Optimal forcing waveforms ($p = 1.1$): (a) $(\Delta\phi, \lambda) = (-\pi, 0)$ and (b) $(\Delta\phi, \lambda) = (-1.2720412, 0.7924492)$.

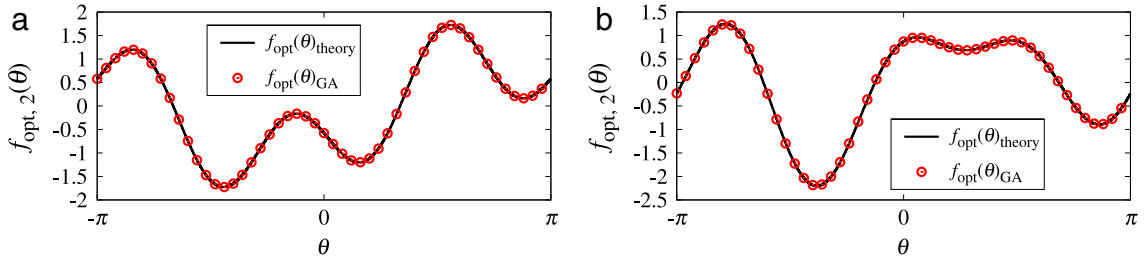

Fig. 10. Optimal forcing waveforms ($p = 2$): (a) $(\Delta\phi, \lambda) = (-\pi, 0)$ and (b) $(\Delta\phi, \lambda) = (-1.3864149, 0.0)$.

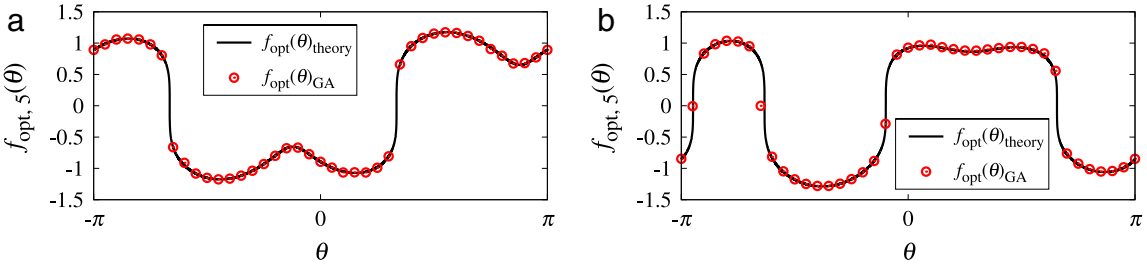

Fig. 11. Optimal forcing waveforms ($p = 5$): (a) $(\Delta\phi, \lambda) = (-\pi, 0)$ and (b) $(\Delta\phi, \lambda) = (-1.4058325, -0.4169387)$.

reduces to the phase equation (2), which enables our optimization methods to be applicable to such systems. We note that a variety of forcing strategies and obtained phase sensitivity functions in [43] are important for designing controls in such systems. (v) Controlling intrinsic localized modes in oscillator arrays: There has been steady progress in research on intrinsic localized vibrational modes (ILMs), both experimentally and theoretically [44–46]. Similarly to the above case of (iv), these ILMs could possibly be regarded as limit cycles in high-dimensional phase space, and in such a situation, we expect it is rather straightforward to apply the results here for controlling such ILMs, as the dynamics of periodically forced ILMs is effectively reduced to Eq. (2).

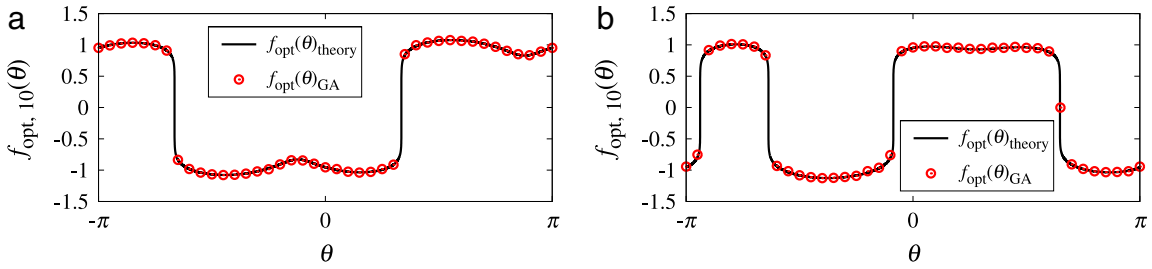

Fig. 12. Optimal forcing waveforms ($p = 10$): (a) $(\Delta\phi, \lambda) = (-\pi, 0)$ and (b) $(\Delta\phi, \lambda) = (-1.4225536, -0.5477614)$.

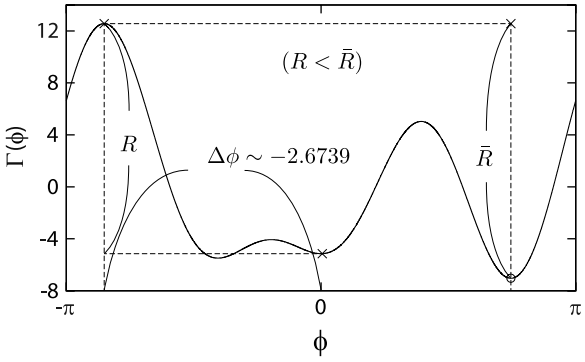

Fig. 13. $\Gamma(\phi)$ for solution 3 ($p = 1.01$).

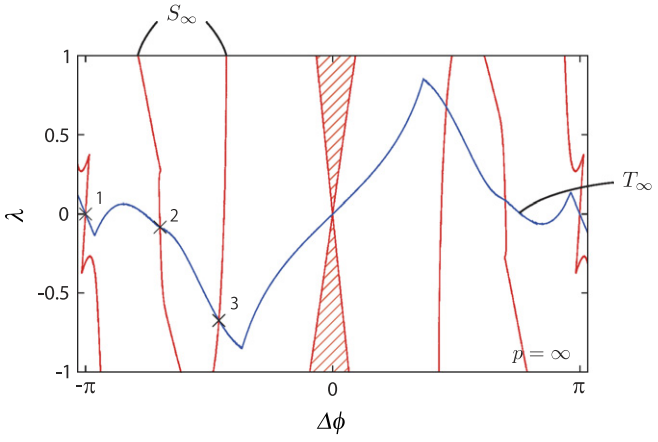

Fig. 14. Solution curve S_∞ of Eq. (69a) and solution curve T_∞ of Eq. (69b) ($p = \infty$).

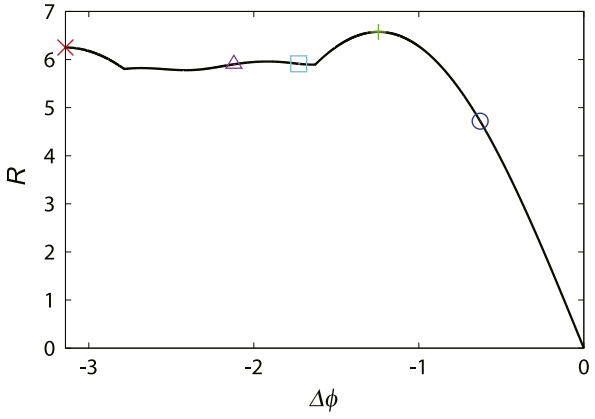

Fig. 16a. Theoretical prediction of $R(\Delta\phi)$. The ×, +, ○, △, and □ symbols here correspond to the datasets shown in Fig. 17.

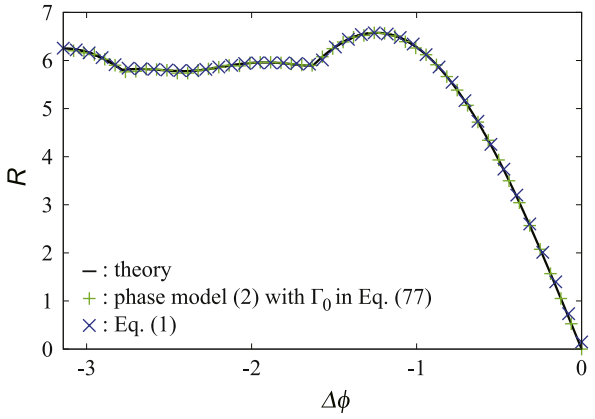

Fig. 16b. $R(\Delta\phi)$ obtained from numerical simulations perfectly match the theoretical prediction. The width and amplitude of the pulses are fixed at 0.07 and 1.14 respectively.

Another challenge still remains to us: to determine whether ILMs in conservative systems (*e.g.*, discrete breathers) can be reduced to a phase description such as Eq. (2). This idea seems rather reasonable, since stable ILMs (elliptic breathers) in finite-dimensional Hamiltonian systems are generically characterized as periodic solutions in the center of KAM tori [47], and the dynamics around such periodic solutions would be reduced to the phase coordinate, at least formally, although an isochrone cannot be generally expected [K. Yoshimura (Personal communication)]. Thereby, the (formal) phase description of Eq. (2) combined with the obtained theory here would provide a new framework for

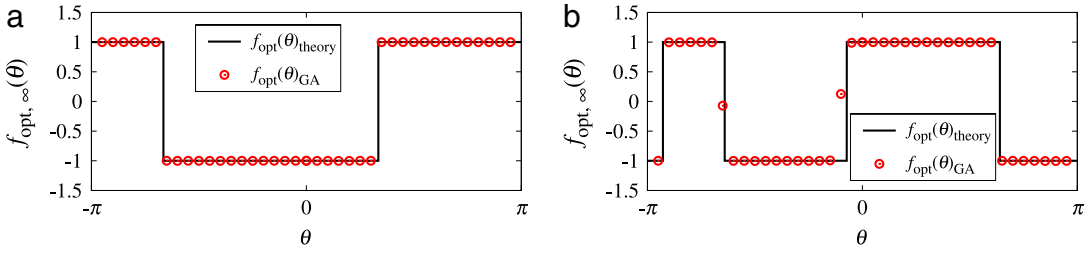

Fig. 15. Optimal forcing waveforms ($p = \infty$): (a) $(\Delta\phi, \lambda) = (-\pi, 0)$ and (b) $(\Delta\phi, \lambda) = (-1.4456283, -0.6738817)$. Here $f_{\mathrm{opt}}(\theta)_{\mathrm{theory}}$ and $f_{\mathrm{opt}}(\theta)_{\mathrm{GA}}$ respectively indicate the results from the theoretical prediction Eq. (32) and a direct GA search.

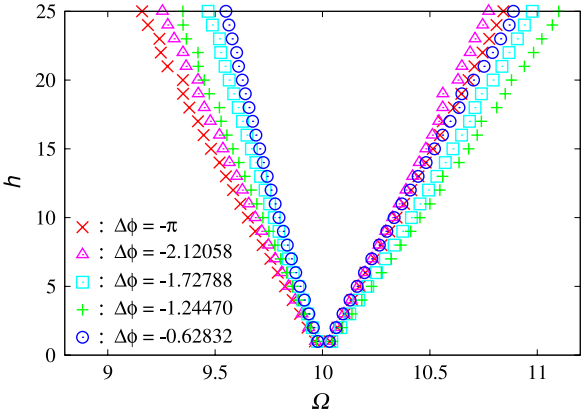

Fig. 17. Arnold tongues for five different impulsive forcings, which correspond to the +, ∘, △, and □ predictions in Fig. 16a. Here Ω and h are the forcing frequency and the amplitude of pulses, respectively. The width of pulses is fixed at 0.07.

controlling discrete breathers, which gives a hint for understanding emerging interesting experimental results such as [48].

8. Proofs of lemmas

8.1. Proof of Lemma 1

First, we verify that $f_{*,\,p}$ in Eq. (13) gives the *ideal* solution; the particular function given by Eq. (13) is a special case of the functions given by (12) which satisfy the equality condition of Hölder's inequality in Eq. (9). In addition, the constraint (4), $\|f_{*,\,p}\|_p = M$, is satisfied, as we have already plugged $\|f\|_p = M$ into Eq. (9).

Next, we verify that the *ideal* solution (13) is a uniquely obtained, by showing the construction of (13) from Eq. (12), which is as follows. $f_{*,\,p}$ in Eq. (13) should satisfy $\langle f_{*,\,p}\, g\rangle = \langle |f_{*,\,p}\, g|\rangle$ in Eq. (9). This requires $f_{*,\,p}(\theta)g(\theta) \geq 0$ a.e. on S. On the other hand, $f_{*,\,p}(\theta)g(\theta) = M\sigma(\theta)g(\theta)\left(\frac{|g(\theta)|}{\|g\|_q}\right)^{\frac{1}{p'}}$, from Eq. (12). Then, $\sigma(\theta)g(\theta)$ has to be a non-negative function, since $M\left(\frac{|g(\theta)|}{\|g\|_q}\right)^{\frac{1}{p'}} \geq 0$ and $f_{*,\,p}\, g$ is a non-negative function. Thus, $\sigma(\theta) = \pm 1$ is uniquely determined as $\sigma(\theta) = \mathrm{sgn}[g(\theta)]$, resulting in Eq. (13). ■

8.2. Proof of Lemma 2

If we assume that the *ideal* solution (13) for m:n entrainment exists, then this requires the equality condition $r|f(n\theta)|^p = s\,|g(m\theta)|^q$ to hold. But this condition is not satisfied in general, except for the trivial case $g(\theta) \equiv$ constant, since f and g are periodic functions with different periods. (Thus, it is now clear that the only possibility for realizing (13) is in the case of $m = n$, namely 1:1 entrainment.) In addition, no other *ideal* solutions can exist without (13) for a given g, due to the uniqueness of the *ideal* solution (13) as shown in Lemma 1. ■

8.3. Proof of Lemma 3

[**Case of** $p \to \infty$ $(p' \to \infty)$] From the assumption (14), it is obvious that $0 \leq |g(\theta)|/\|g\|_q < \infty$, and hence, as $p' \to \infty$,

$$\left(\frac{|g(\theta)|}{\|g\|_q}\right)^{\frac{1}{p'}} \to \begin{cases} 1, & \text{for } |g(\theta)| > 0 \\ 0, & \text{for } |g(\theta)| = 0. \end{cases} \tag{38}$$

Thus, taking the limit of (38) in Eq. (13), Eq. (15) is obtained.

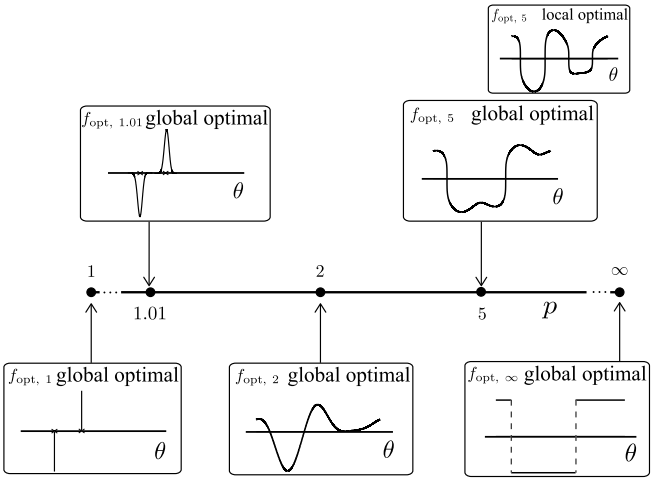

Fig. 18. Overview of optimal forcings for various $p \in [1, \infty]$ obtained for the Hodgkin–Huxley phase model with Eq. (37).

[**Case of** $p \to 1$ $(p' \to +0)$] The limiting value of $(|g(\theta)|/\|g\|_q)^{\frac{1}{p'}}$ in Eq. (13) is obtained by the following calculations at $\theta = \theta_*$ and at $\theta \neq \theta_*$. First, rescaling $|g(\theta)|/\|g\|_q$ with $\bar{g}(\theta) = g(\theta)/|g(\theta_*)|$, we have $|\bar{g}(\theta_*)|^{\frac{1}{p'}} = 1$ (for any p'), and for any θ we have:

$$\left(\frac{|g(\theta)|}{\|g\|_q}\right)^{\frac{1}{p'}} = \left(\frac{|C\bar{g}(\theta)|}{\|C\bar{g}\|_q}\right)^{\frac{1}{p'}} = \frac{|\bar{g}(\theta)|^{\frac{1}{p'}}}{\langle |\bar{g}(\theta)|^{1+\frac{1}{p'}}\rangle^{\frac{1}{1+p'}}} = \left(\frac{|\bar{g}(\theta)|}{\|\bar{g}\|_q}\right)^{\frac{1}{p'}}, \tag{39}$$

where C denotes $|g(\theta_*)|$ $(<\infty)$. Since we have assumed θ_* to have 0 measure in Section 4.2, from $|\bar{g}(\theta)| < 1$ and $\frac{1}{1+p'} \to 1$ $(p' \to +0)$, we have $|\bar{g}(\theta)|^{1+\frac{1}{p'}} \to +0$ a.e. on S, resulting in $\langle |\bar{g}(\theta)|^{1+\frac{1}{p'}}\rangle^{\frac{1}{1+p'}} \to +0$ $(p' \to +0)$. Thus, for $\theta = \theta_*$ we obtain $\left(\frac{|g(\theta_*)|}{\|g\|_q}\right)^{\frac{1}{p'}} \to +\infty$ $(p' \to +0)$ from Eq. (39).

In contrast, for $\theta \neq \theta_*$, we have $\|\bar{g}\|_q \to \|\bar{g}\|_\infty = 1$ $(q \to +\infty)$,[2] and $\bar{g}(\theta) < 1$. This implies $\frac{|\bar{g}(\theta)|}{\|\bar{g}\|_q} \to |\bar{g}(\theta)| < 1$ $(q \to +\infty)$. Then, by taking the logarithm of Eq. (39), $\log\left[\left(\frac{|\bar{g}(\theta)|}{\|\bar{g}\|_q}\right)^{\frac{1}{p'}}\right] = (q-1)\log\left(\frac{|\bar{g}(\theta)|}{\|\bar{g}\|_q}\right) \to -\infty$ $(q \to +\infty)$, and hence $\left(\frac{|g(\theta)|}{\|g(\theta)\|_q}\right)^{\frac{1}{p'}} \to +0$ $(p' \to +0)$. Thus, from these calculations, we obtain the limit of (16). ■

8.4. Proof of Lemma 4

First, $\|fg\|_1$ is maximized by $f_{*,\,\infty}$, since

$$\|f_{*,\,\infty}\, g\|_1 = \langle M\mathrm{sgn}[g(\theta)]\; g(\theta)\rangle = M\,\langle |g(\theta)|\rangle = M\|g\|_1. \tag{40}$$

Second, the unique representation of this *ideal* solution $f_{*,\,\infty}$ is shown by proof by contradiction, as follows. Suppose another *ideal* solution $\bar{f}_{*,\,\infty}$ exists and it maximizes $\|fg\|_1$, *i.e.*, $\|\bar{f}_{*,\,\infty}\, g\|_1 = M\|g\|_1$. Then, for any given $g \in L^1(S)$, the following is satisfied:

$$\|f_{*,\,\infty}\, g\|_1 - \|\bar{f}_{*,\,\infty}\, g\|_1 = 0. \tag{41}$$

[2] To be more precise, here we have assumed $||\bar{g}||_r < \infty$ for some $r < \infty$. This assumption is quite natural in our context, as we can set $r = 2$, for instance, and then $||\bar{g}||_q \to ||\bar{g}||_\infty$ $(q \to \infty)$ follows. See [29] on p. 71 for an outline of the proof.

Now, using the identities $f_{*,\infty}(\theta)g(\theta) = M\mathrm{sgn}[g(\theta)]\cdot g(\theta) \geq 0$ and $|g(\theta)| = f_{*,\infty}(\theta)g(\theta)/M$, we obtain $|f_{*,\infty}(\theta)g(\theta)| - |\bar{f}_{*,\infty}(\theta)g(\theta)| = f_{*,\infty}(\theta)g(\theta) - |\bar{f}_{*,\infty}(\theta)||g(\theta)|$ and $f_{*,\infty}(\theta)g(\theta) - |\bar{f}_{*,\infty}(\theta)||g(\theta)| = f_{*,\infty}(\theta)g(\theta) - \frac{|\bar{f}_{*,\infty}(\theta)|}{M}f_{*,\infty}(\theta)g(\theta)$, respectively, resulting in the equality

$$|f_{*,\infty}(\theta)g(\theta)| - |\bar{f}_{*,\infty}(\theta)g(\theta)| = f_{*,\infty}(\theta)g(\theta) - \frac{|\bar{f}_{*,\infty}(\theta)|}{M}f_{*,\infty}(\theta)g(\theta). \quad (42)$$

Plugging Eq. (42) into the lhs of Eq. (41) and using $|g(\theta)| = f_{*,\infty}(\theta)g(\theta)/M$, Eq. (41) is rewritten as

$$\left\langle \left(1 - \frac{|\bar{f}_{*,\infty}(\theta)|}{M}\right) f_{*,\infty}(\theta)\, g(\theta) \right\rangle = \langle (M - |\bar{f}_{*,\infty}(\theta)|)|g(\theta)|\rangle = 0. \quad (43)$$

Now, keeping $|\bar{f}_{*,\infty}(\theta)| \leq M$ and the assumption that $g(\theta) \neq 0$, a.e. on S in mind, Eq. (43) implies

$$|\bar{f}_{*,\infty}(\theta)| = M, \quad \text{or equivalently} \quad \bar{f}_{*,\infty}(\theta) = M\sigma(\theta), \ \text{a.e. on } S. \quad (44)$$

However, among such functions $\bar{f}_{*,\infty}$ having either M or $-M$ values, it is clear that $M\mathrm{sgn}[g(\theta)]$ ($=f_{*,\infty}$) only makes $\langle fg\rangle$ maximal. Thus, no $\bar{f}_{*,\infty}$ can exist except for $f_{*,\infty}$, and thus the uniqueness of the *ideal* solution $f_{*,\infty}$ is verified.

Finally, similarly to the argument in Lemma 2, this unique, *ideal* solution (18) is realized only for 1:1 entrainment, since $f_{*,\infty}$ and g in Eq. (18) must have the same period. ■

8.5. Proof of Lemma 5

In Eqs. (21) and (22), $\Delta \in L^1(S)$ and $f_{*,1} \in L^1(S)$, respectively, and this $f_{*,1}$ satisfies $\|f_{*,1}\|_1 = M$. Now, $\langle f_{*,1}\, g\rangle \to M\|g\|_\infty$ ($\epsilon \to +0$) since $\langle f_{*,1}\, g\rangle = M\langle \sum_{i=1}^{n} \mathrm{sgn}[g(\bar{\theta}_i)]\Delta(\theta - \bar{\theta}_i)g(\theta)\rangle \to M|g(\bar{\theta}_i)| = M\|g\|_\infty$. The proof of this limit is given in Appendix E as (a). ■

9. Proofs of theorems

9.1. Proof of Theorem 1

Here, we outline the proof. The assumption in Lemma 1 (*i.e.*, $f \in L^p(S)$, $g \in L^q(S)$) is satisfied by the constraint $\|f\|_p = M$ and assumption (i) in Theorem 1. Another assumption (*i.e.*, $\|g\|_q$ is not affected by f) is satisfied since $\Delta\phi$ and λ are undetermined free parameters at this stage. Then, using Lemma 1, we start from the ideal solution (13) with Eq. (24) which reduces down to the finite dimensional optimization problem of H with two variables $\Delta\phi$ and λ in Eq. (31). This optimization of H is possible, owing to the following facts. First, from assumption (iii) in Theorem 1, H has only isolated optimal points. Second, from assumptions (i), (ii), and (iv), the derivatives $\frac{\partial^2 H}{\partial \Delta\phi^2}$, $\frac{\partial^2 H}{\partial \Delta\phi \partial\lambda}$, $\frac{\partial^2 H}{\partial\lambda \partial \Delta\phi}$, and $\frac{\partial^2 H}{\partial\lambda^2}$ are continuous in the neighborhood of the optimal points; this is directly verified by the (ϵ, δ)-definition of limit (See Appendix F for more details.), using the following (a) and (b): (a) all required derivatives of H are explicitly given as in Eq. (51), and (b) some integrals in Eq. (51) become singular, but all of them have finite values, and the contribution from singular points are on the order of ϵ^β (as estimated in Appendix D).

Then, as the next step, we obtain the necessary and sufficient conditions for the existence of the optimal solutions of H in Section 9.1.1. Finally, using these conditions, we characterize the optimal forcings, and we verify that the global optimal forcing $f_{\mathrm{opt},\, p}$ indeed maximizes the locking range in the original Eqs. (2) and (3), in Section 9.1.2.

9.1.1. Necessary and sufficient conditions of optimal solutions $(\Delta\phi_*, \lambda_*)$

Note that $\left(\frac{\partial G}{\partial \Delta\phi}, \frac{\partial G}{\partial\lambda}\right) \neq \mathbf{0}$ is always satisfied, since $\frac{\partial G}{\partial\lambda} > 0$ as obtained below in Eq. (49). Then, the Lagrange multiplier rule is applied, which implies that some value of the μ (which can be 0) in Eq. (31) satisfying the associated optimization problem exists and that the associated optimal solution $(\Delta\phi_*, \lambda_*)$ to Eq. (31) satisfies

$$\left(\frac{\partial H}{\partial \Delta\phi}, \frac{\partial H}{\partial\lambda}\right) = \mathbf{0}, \quad (45)$$

if it exists. Namely, candidates of the optimal solution to the optimization of (31) are obtained by solving Eq. (45) with the associated constraint $G(\Delta\phi, \lambda) = 0$ for $\Delta\phi_*, \lambda_*$, and μ_*; the derivation process is as follows.

We start from abbreviating $\frac{p'+1}{p'}$ and $\frac{1}{p'}$, respectively, as $\frac{p'+1}{p'} \equiv \alpha > 0$ and $\frac{1}{p'} \equiv \beta > 0$, as in Eq. (25). Then, the derivatives of $F(\Delta\phi, \lambda)$ in Eq. (28) are obtained as

$$\frac{\partial F}{\partial \Delta\phi} = \alpha \left\langle \mathrm{sgn}[\bar{Z}(\theta) + \lambda]|\bar{Z}(\theta) + \lambda|^\beta Z'(\theta + \Delta\phi)\right\rangle \equiv F_1(\Delta\phi, \lambda) \quad (46)$$

$$\frac{\partial F}{\partial\lambda} = \alpha \left\langle \mathrm{sgn}[\bar{Z}(\theta) + \lambda]|\bar{Z}(\theta) + \lambda|^\beta \right\rangle = \alpha G \equiv F_2(\Delta\phi, \lambda). \quad (47)$$

Likewise, the derivatives of $G(\Delta\phi, \lambda)$ in Eq. (30) are obtained as

$$\frac{\partial G}{\partial \Delta\phi} = \beta \left\langle |\bar{Z}(\theta) + \lambda|^{\beta-1} Z'(\theta + \Delta\phi)\right\rangle, \quad (48)$$

$$\frac{\partial G}{\partial\lambda} = \beta \left\langle |\bar{Z}(\theta) + \lambda|^{\beta-1}\right\rangle > 0. \quad (49)$$

For the derivation of Eqs. (46)–(49), see Appendix B. Note that in Eq. (47) $F_2(\Delta\phi, \lambda) = \alpha \left\langle \mathrm{sgn}(\bar{Z}(\theta) + \lambda)|\bar{Z} + \lambda|^\beta\right\rangle = 0$ is simply the constraint $G(\Delta\phi, \lambda) = 0$. Since in Eq. (45) we have $\frac{\partial H}{\partial\lambda} = \frac{\partial F}{\partial\lambda} + \mu\frac{\partial G}{\partial\lambda} = 0$, and $\frac{\partial F}{\partial\lambda} = \alpha G(\Delta\phi, \lambda) = 0$ and $\frac{\partial G}{\partial\lambda} > 0$ follow from the above arguments, μ_* is uniquely determined as $\mu_* = 0$. (This sounds a bit contradictory, as the μG term vanishes in Eq. (31) if $\mu = \mu_* = 0$; however, for $\mu_* = 0$, Eq. (45) reduces to $F_1(\Delta\phi, \lambda) = F_2(\Delta\phi, \lambda) = 0$, and the solutions to this automatically satisfy the constraint (5). Hence, the situation here does not contradict the result from the Lagrange multiplier rule.) Thus, the candidates for optimal solutions are obtained from $F_1 = F_2 = 0$.[3]

Now we are in position to distinguish optimal solutions from non-optimal ones. For this purpose, the so-called bordered Hessian matrix of $\mathcal{H}$ [31] is introduced as

$$\mathcal{H}(H) = \begin{bmatrix} 0 & \mathcal{H}_{12} & \mathcal{H}_{13} \\ \mathcal{H}_{21} & \mathcal{H}_{22} & \mathcal{H}_{23} \\ \mathcal{H}_{31} & \mathcal{H}_{32} & \mathcal{H}_{33} \end{bmatrix}, \quad (50)$$

whose elements are given by

$$\mathcal{H}_{12} = \mathcal{H}_{21} = \frac{\partial G}{\partial \Delta\phi} = \beta \left\langle |\bar{Z}(\theta) + \lambda|^{\beta-1} Z'(\theta + \Delta\phi)\right\rangle, \quad (51a)$$

$$\mathcal{H}_{13} = \mathcal{H}_{31} = \frac{\partial G}{\partial\lambda} = \beta \left\langle |\bar{Z}(\theta) + \lambda|^{\beta-1}\right\rangle > 0, \quad (51b)$$

[3] In this particular problem, if we utilize the convenient property that $\frac{\partial F}{\partial\lambda} = 0$ is equivalent to the constraint $G = 0$, then the problem reduces to the optimization of F. However, in more general situations beyond our particular problem, this convenient property does not necessarily hold. Therefore, here we optimize H instead of F to keep the method general.

$$\mathcal{H}_{22} = \frac{\partial^2 F}{\partial \Delta\phi^2} = \alpha\beta\left\langle |\bar{Z}(\theta)+\lambda|^{\beta-1} Z'(\theta+\Delta\phi)^2\right\rangle + \alpha\left\langle \mathrm{sgn}[\bar{Z}(\theta)+\lambda]|\bar{Z}(\theta)+\lambda|^{\beta} Z''(\theta+\Delta\phi)\right\rangle, \quad (51c)$$

$$\mathcal{H}_{23} = \frac{\partial^2 F}{\partial \Delta\phi \partial\lambda} = \alpha\beta\left\langle |\bar{Z}(\theta)+\lambda|^{\beta-1} Z'(\theta+\Delta\phi)\right\rangle = \alpha\mathcal{H}_{12}, \quad (51d)$$

$$\mathcal{H}_{32} = \frac{\partial^2 F}{\partial\lambda\partial\Delta\phi} = \alpha\frac{\partial}{\partial\Delta\phi}\left\langle \mathrm{sgn}[\bar{Z}(\theta)+\lambda]|\bar{Z}(\theta)+\lambda|^{\beta}\right\rangle = \alpha\beta\left\langle |\bar{Z}(\theta)+\lambda|^{\beta-1} Z'(\theta+\Delta\phi)\right\rangle = \alpha\mathcal{H}_{12}, \quad (51e)$$

$$\mathcal{H}_{33} = \frac{\partial^2 F}{\partial\lambda^2} = \alpha\frac{\partial}{\partial\lambda}\left\langle \mathrm{sgn}[\bar{Z}(\theta)+\lambda]|\bar{Z}(\theta)+\lambda|^{\beta}\right\rangle = \alpha\beta\left\langle |\bar{Z}(\theta)+\lambda|^{\beta-1}\right\rangle = \alpha\mathcal{H}_{13} > 0. \quad (51f)$$

See Appendix B, for the outline of these derivations.

The Hessian $|\mathcal{H}(H)|$ is then obtained as

$$|\mathcal{H}(H)| = \mathcal{H}_{13}(\alpha\mathcal{H}_{12}{}^2 - \mathcal{H}_{13}\mathcal{H}_{22}), \quad (52)$$

which turns out to be particularly useful because the solution $(\Delta\phi_*, \lambda_*)$ to $F_1(\Delta\phi,\lambda) = F_2(\Delta\phi,\lambda) = 0$ becomes maximal if it satisfies $|\mathcal{H}(H)| > 0$, and it becomes minimal if $|\mathcal{H}(H)| < 0$ [31]. Hence, from the above calculations, the optimal solution $(\Delta\phi, \lambda)$ to Eq. (28) under the charge-balance constraint (29) is found to exist, if the following conditions are satisfied:

$$\left\langle \mathrm{sgn}[\bar{Z}(\theta)+\lambda]|\bar{Z}(\theta)+\lambda|^{\beta} Z'(\theta+\Delta\phi)\right\rangle = 0\ (=\alpha^{-1}F_1), \quad (53)$$

$$\left\langle \mathrm{sgn}[\bar{Z}(\theta)+\lambda]|\bar{Z}(\theta)+\lambda|^{\beta}\right\rangle = 0\ (=\alpha^{-1}F_2), \quad (54)$$

$$|\mathcal{H}(H)| = \mathcal{H}_{13}(\alpha\mathcal{H}_{12}^2 - \mathcal{H}_{13}\mathcal{H}_{22}) > 0. \quad (55)$$

We note here, for this optimal solution, that the inequality

$$\left\langle \mathrm{sgn}[\bar{Z}(\theta)+\lambda]|\bar{Z}(\theta)+\lambda|^{\beta} Z''(\theta+\Delta\phi)\right\rangle < 0 \quad (56)$$

is automatically satisfied, which will be key for characterizing the optimality of $\Gamma(\phi)$ later, in Section 9.1.2. For the derivation of Eq. (56), see Appendix C.

Finally, we note that all the integrals involving $|\bar{Z}(\theta)+\lambda|^{\beta-1}$ in Eq. (51) can be singular when $2 < p < \infty$, *i.e.*, $0 < \beta = \frac{1}{p'} = \frac{1}{p-1} < 1$, because $\bar{Z}(\theta)+\lambda$ may possibly have zeros θ_* and $|\bar{Z}(\theta)+\lambda|^{\beta-1}$ becomes infinite at $\theta = \theta_*$. However, all such integrals have finite values if $\bar{Z}(\theta)$ is twice differentiable and $\bar{Z}'(\theta_*) \neq 0$ for every θ_*, for instance. For the proof, see Appendix D.

9.1.2. Symmetry of solutions $(\Delta\phi, \lambda)$ and verification of maximal locking range $R[f]$

Here we focus on the symmetry of the solutions $(\Delta\phi, \lambda)$ to Eqs. (53)–(55), as follows. First, we note that there is a symmetry both in F and G: $F(\Delta\phi,\lambda) = F(-\Delta\phi,-\lambda)$ in Eq. (28) and $G(\Delta\phi,\lambda) = G(-\Delta\phi,-\lambda)$ in Eq. (30) for any $\Delta\phi$ and λ. Then, if $(\Delta\phi_*, \lambda_*)$ is a solution to Eqs. (53) and (54), $(-\Delta\phi_*, -\lambda_*)$ is also a solution to Eqs. (53) and (54). For this pair of solutions $(\Delta\phi,\lambda) = (\pm\Delta\phi_*, \pm\lambda_*)$, $g(\theta)$ and $f_{\mathrm{opt},\,p}(\theta)$ are respectively given by

$$g(\theta) = \pm[\bar{Z}(\theta)+\lambda_*], \quad (57a)$$

$$f_{\mathrm{opt},\,p}(\theta) = \pm M\mathrm{sgn}\left[\bar{Z}(\theta)+\lambda_*\right]\left(\frac{|\bar{Z}(\theta)+\lambda_*|}{\|\bar{Z}(\theta)+\lambda_*\|_q}\right)^{\beta}, \quad (57b)$$

where $\bar{Z}(\theta) = Z(\theta+\Delta\phi_*) - Z(\theta)$. Thus, $\langle f_{\mathrm{opt},\,p}\, g\rangle$ has the same value for both solutions.

The reason for this coincidence is now understood as follows. The pair of forcings in Eq. (57b) corresponding to the $\pm$ signs have a mutually inverted relationship across the θ axis in their graphs, and hence the associated Γ's have the same symmetry, since $\Gamma(\phi) = \frac{1}{2\pi}\langle Z(\theta+\phi) f_{\mathrm{opt},\,p}(\theta)\rangle$. Therefore, the locking range $\frac{1}{2\pi}\langle f_{\mathrm{opt},\,p}\, g\rangle \sim F(\Delta\phi,\lambda)$, *i.e.*, the maximum of $\Gamma(\phi)$ – the minimum of $\Gamma(\phi)$, are the same for both forcings in (57b). Therefore, since we have assumed this $F(\Delta\phi,\lambda)$ to be maximized at $(\Delta\phi,\lambda) = (\Delta\phi_*,\lambda_*)$, it is simultaneously maximized at $(\Delta\phi,\lambda) = (-\Delta\phi_*,-\lambda_*)$, due to the symmetry of $F(-\Delta\phi,-\lambda) = F(\Delta\phi,\lambda)$. Thus, $|\mathcal{H}(H(-\Delta\phi_*,-\lambda_*))| > 0$ (or ≤ 0) has to be satisfied if $|\mathcal{H}(H(\Delta\phi_*,\lambda_*))| > 0$ (or ≤ 0).

Finally, we will verify the original definition of Γ as shown in Fig. 1 as follows: the global optimal forcing $f_{\mathrm{opt},\,p}$ indeed maximizes Γ at ϕ_+ and minimizes Γ at ϕ_-, respectively. Here, we note that $\Gamma(\phi)$ is twice differentiable, from assumption (i) in Theorem 1 and the fact that $f_{\mathrm{opt},\,p}$ in (57b) is continuous. Also, the following has to be satisfied, as shown in Fig. 1 in Section 2:

$$\Gamma'(\phi_\pm) = 0, \qquad \Gamma''(\phi_+) < 0, \quad \text{and} \quad \Gamma''(\phi_-) > 0. \quad (58)$$

First, from Eqs. (3) and (57b), Γ is now

$$\Gamma(\phi) = \frac{1}{2\pi}\left\langle Z(\theta+\phi) f_{\mathrm{opt},p}(\theta)\right\rangle = C\langle Z(\theta+\phi)\,\mathrm{sgn}\left[\bar{Z}(\theta)+\lambda\right]|\bar{Z}(\theta)+\lambda|^{\beta}\rangle, \quad (59)$$

where $C = \frac{M}{2\pi}\|\bar{Z}(\theta)+\lambda\|_q^{-\beta} > 0$. Furthermore, $\Gamma'(\phi)\left(=\frac{d\Gamma(\phi)}{d\phi}\right)$ and $\Gamma''(\phi)\left(=\frac{d^2\Gamma(\phi)}{d\phi^2}\right)$ are respectively $\Gamma'(\phi) = C\left\langle Z'(\theta+\phi)\,\mathrm{sgn}\,[\bar{Z}(\theta)+\lambda]\,|\bar{Z}(\theta)+\lambda|^{\beta}\right\rangle$ and $\Gamma''(\phi) = C\left\langle Z''(\theta+\phi)\,\mathrm{sgn}[\bar{Z}(\theta)+\lambda]\,|\bar{Z}(\theta)+\lambda|^{\beta}\right\rangle$, since $\bar{Z}(\theta) = Z(\theta+\phi_+) - Z(\theta+\phi_-)$ does not depend on ϕ. Thus, for $(\Delta\phi,\lambda) = (\Delta\phi_*,\lambda_*)$, $\Gamma'(\phi_+)$ and $\Gamma''(\phi_+)$ respectively should satisfy

$$\Gamma'(\phi_+) = C\langle Z'(\theta+\phi_+)\,\mathrm{sgn}[\bar{Z}(\theta)+\lambda_*]\,|\bar{Z}(\theta)+\lambda_*|^{\beta}\rangle = C\langle \mathrm{sgn}[Z(\theta+\Delta\phi_*) - Z(\theta)+\lambda_*]\,|Z(\theta+\Delta\phi_*) - Z(\theta)+\lambda_*|^{\beta} Z'(\theta+\Delta\phi_*)\rangle = 0, \quad (60a)$$

$$\Gamma''(\phi_+) = C\langle Z''(\theta+\phi_+)\,\mathrm{sgn}[\bar{Z}(\theta)+\lambda_*]\,|\bar{Z}(\theta)+\lambda_*|^{\beta}\rangle = C\langle \mathrm{sgn}[Z(\theta+\Delta\phi_*) - Z(\theta)+\lambda_*]\,|Z(\theta+\Delta\phi_*) - Z(\theta)+\lambda_*|^{\beta} Z''(\theta+\Delta\phi_*)\rangle < 0. \quad (60b)$$

Second, these conditions (60a) and (60b) are automatically satisfied, as we have already obtained them in Eqs. (53) and (56) for $(\Delta\phi,\lambda) = (\Delta\phi_*,\lambda_*)$. The same holds true for $\Gamma'(\phi_-)$ and $\Gamma''(\phi_-)$; that is, for $(\Delta\phi,\lambda) = (\Delta\phi_*,\lambda_*)$, $\Gamma'(\phi_-)$ and $\Gamma''(\phi_-)$ in Eq. (58) should satisfy

$$\Gamma'(\phi_-) = C\left\langle Z'(\theta+\phi_-)\,\mathrm{sgn}[\bar{Z}(\theta)+\lambda_*]\,|\bar{Z}(\theta)+\lambda_*|^{\beta}\right\rangle = C\left\langle \mathrm{sgn}[Z(\theta+\Delta\phi_*) - Z(\theta)+\lambda_*]\,|Z(\theta+\Delta\phi_*) - Z(\theta)+\lambda_*|^{\beta} Z'(\theta)\right\rangle = 0, \quad (61a)$$

$$\Gamma''(\phi_-) = C\left\langle Z''(\theta+\phi_-)\,\mathrm{sgn}[\bar{Z}(\theta)+\lambda_*]\,|\bar{Z}(\theta)+\lambda_*|^{\beta}\right\rangle = C\left\langle \mathrm{sgn}[Z(\theta+\Delta\phi_*) - Z(\theta)+\lambda_*]\,|Z(\theta+\Delta\phi_*) - Z(\theta)+\lambda_*|^{\beta} Z''(\theta)\right\rangle > 0, \quad (61b)$$

where Eqs. (61a) and (61b) are simply Eqs. (53) and (56) for $(\Delta\phi,\lambda) = (-\Delta\phi_*,-\lambda_*)$, respectively, which are obtained by replacing $\theta - \Delta\phi_*$ with θ in Eqs. (53) and (56).

Hence, from the relationships between Eqs. (53), (56), and (58), it is concluded that for any $(\Delta\phi_*,\lambda_*)$ satisfying Eqs. (53)–(55), $f_{\mathrm{opt},\,p}$ in Eq. (26) is indeed global possible optimal forcing, whose locking range $\frac{1}{2\pi}\langle f_{\mathrm{opt},\,p}\, g\rangle$ is given as $\frac{M}{2\pi}\langle(\bar{Z}+\lambda)^{\alpha}\rangle^{\frac{1}{\alpha}} = \frac{M}{2\pi}F(\Delta\phi_*,\lambda_*)^{\frac{1}{\alpha}}$. As M and α are given constants here, the global optimal forcing is realized at $(\Delta\phi_*,\lambda_*) = (\overline{\Delta\phi_*}, \overline{\lambda_*})$, for which

$F(\overline{\Delta\phi_*}, \bar{\lambda}_*)$ becomes the largest among all $F(\Delta\phi_*, \lambda_*)$'s. (end of the proof of Theorem 1) ■

Here, we note that the above argument for $1 < p < \infty$ becomes much simpler for the specific case of $p = 2$, as follows. In this case, Eqs. (53) and (54) respectively become

$$\langle [Z(\theta + \Delta\phi) - Z(\theta) + \lambda] Z'(\theta + \Delta\phi) \rangle = 0, \tag{62}$$

$$\langle Z(\theta + \Delta\phi) - Z(\theta) + \lambda \rangle = 0. \tag{63}$$

Since $\langle Z(\theta + \Delta\phi) - Z(\theta) \rangle = \langle Z(\theta + \Delta\phi) \rangle - \langle Z(\theta) \rangle = 0$, Eq. (63) gives $\lambda = 0$, and Eq. (62) becomes $\langle [Z(\theta + \Delta\phi) - Z(\theta)] Z'(\theta + \Delta\phi) \rangle = \frac{1}{2} \left[Z(\theta + \Delta\phi)^2 \right]_0^{2\pi} - \langle Z(\theta) Z'(\theta + \Delta\phi) \rangle = 0$, *i.e.*, $\langle Z(\theta) Z'(\theta + \Delta\phi) \rangle = 0$, which is a condition determining $\Delta\phi$, as appeared in [25] via variational calculus. Also, in this case Eq. (56) becomes $\langle [Z(\theta + \Delta\phi) - Z(\theta)] Z''(\theta + \Delta\phi) \rangle < 0$, which is obtained by the Cauchy–Schwarz inequality in [25].

9.2. Outline of proof of Theorem 2

As the proof is quite similar to that of Theorem 1, we start by listing the differences. First, the singular integrals appearing in Eq. (51) do not appear in this case, $p = \infty$ (as shown in (68)). Thus, assumption (i) is a bit relaxed. Second, as we see in Eq. (68), a somewhat 'discrete' nature appears in the elements of the bordered Hessian matrix for H_∞: some elements are determined by only the local information of Z' and $\bar{Z}'$ at zeros of $\bar{Z} + \lambda$. This in turn results in the quite simple formula (70) for optimality, via the finite-dimensional Cauchy–Schwarz inequality (73).

The proof and required calculations are outlined as follows. From Eq. (68b), $\left(\frac{\partial G_\infty}{\partial \Delta\phi}, \frac{\partial G_\infty}{\partial \lambda} \right) \neq \mathbf{0}$. From Eq. (68), the continuity of the derivatives of H_∞ is verified, similarly to in Section 9.1. Hence, the Lagrange multiplier rule implies that there exists μ_*, and $\left(\frac{\partial H_\infty}{\partial \Delta\phi}, \frac{\partial H_\infty}{\partial \lambda} \right) = \mathbf{0}$ is satisfied at the optimal solution $(\Delta\phi_*, \lambda_*)$, as mentioned in assumption (iii). Now, μ_* and $(\Delta\phi_*, \lambda_*)$ are determined, following the same procedure as in the case of $1 < p < \infty$ in Section 9.1.1. For this purpose, we require twice-differentiable $Z(\theta)$ and $g(\theta)$ as in assumptions (i) and (ii), which results in

$$\frac{\partial F_\infty}{\partial \Delta\phi} = \langle \mathrm{sgn}[\bar{Z}(\theta) + \lambda] Z'(\theta + \Delta\phi) \rangle, \tag{64}$$

$$\frac{\partial F_\infty}{\partial \lambda} = \langle \mathrm{sgn}[\bar{Z}(\theta) + \lambda] \rangle = G_\infty(\Delta\phi, \lambda), \tag{65}$$

$$\frac{\partial G_\infty}{\partial \Delta\phi} = 2 \sum_{i=1}^{n} \frac{Z'(\theta_i + \Delta\phi)}{|\bar{Z}'(\theta_i)|}, \tag{66}$$

$$\frac{\partial G_\infty}{\partial \lambda} = 2 \sum_{i=1}^{n} \frac{1}{|\bar{Z}'(\theta_i)|} > 0, \tag{67}$$

where θ_i represents the ith root of $\bar{Z}(\theta) + \lambda = 0$ (*i.e.*, θ_* in Theorem 2), and n is the number of the roots (an even number since $\bar{Z}(\theta)$ is periodic and $\bar{Z}'(\theta_i) \neq 0$). The derivation of Eqs. (64)–(67) is given in Appendix B. Similarly to the case of $1 < p < \infty$ in Section 9.1.1, $\mu = \mu_*$ is uniquely determined as $\mu_* = 0$, since $\frac{\partial H_\infty}{\partial \lambda} = \frac{\partial F_\infty}{\partial \lambda} + \mu_* \frac{\partial G_\infty}{\partial \lambda}$, and $\frac{\partial F_\infty}{\partial \lambda} = 0$ and $\frac{\partial G_\infty}{\partial \lambda} > 0$. In addition, $\Delta\phi_*$ and λ_* are determined by $\langle \mathrm{sgn}[\bar{Z}(\theta) + \lambda] Z'(\theta + \Delta\phi) \rangle = 0$ and $\langle \mathrm{sgn}[\bar{Z}(\theta) + \lambda] \rangle = 0$. Now, the bordered Hessian matrix of H_∞ is given by

$$\mathcal{H}_{12} = \mathcal{H}_{21} = \frac{\partial G_\infty}{\partial \Delta\phi} = 2 \sum_{i=1}^{n} \frac{Z'(\theta_i + \Delta\phi)}{|\bar{Z}'(\theta_i)|}, \tag{68a}$$

$$\mathcal{H}_{13} = \mathcal{H}_{31} = \frac{\partial G_\infty}{\partial \lambda} = 2 \sum_{i=1}^{n} \frac{1}{|\bar{Z}'(\theta_i)|} > 0, \tag{68b}$$

$$\mathcal{H}_{22} = \frac{\partial^2 F_\infty}{\partial \Delta\phi^2} = 2 \sum_{i=1}^{n} \frac{Z'(\theta_i + \Delta\phi)^2}{|\bar{Z}'(\theta_i)|} + \langle \mathrm{sgn}[\bar{Z}(\theta) + \lambda] Z''(\theta + \Delta\phi) \rangle, \tag{68c}$$

$$\mathcal{H}_{23} = \frac{\partial^2 F_\infty}{\partial \Delta\phi \partial \lambda} = 2 \sum_{i=1}^{n} \frac{Z'(\theta_i + \Delta\phi)}{|\bar{Z}'(\theta_i)|} = \mathcal{H}_{12}, \tag{68d}$$

$$\mathcal{H}_{32} = \frac{\partial^2 F_\infty}{\partial \lambda \partial \Delta\phi} = 2 \sum_{i=1}^{n} \frac{Z'(\theta_i + \Delta\phi)}{|\bar{Z}'(\theta_i)|} = \mathcal{H}_{12}, \tag{68e}$$

$$\mathcal{H}_{33} = \frac{\partial^2 F_\infty}{\partial \lambda^2} = 2 \sum_{i=1}^{n} \frac{1}{|\bar{Z}'(\theta_i)|} = \mathcal{H}_{13} > 0. \tag{68f}$$

See Appendix B for the outline of these derivations. Hence, the optimal solution $(\Delta\phi, \lambda)$ to Eq. (34) is obtained if and only if it satisfies the following conditions:

$$\langle \mathrm{sgn}[\bar{Z}(\theta) + \lambda] Z'(\theta + \Delta\phi) \rangle = 0, \tag{69a}$$

$$\langle \mathrm{sgn}[\bar{Z}(\theta) + \lambda] \rangle = 0, \tag{69b}$$

$$|\mathcal{H}(H)| = \mathcal{H}_{13}(\mathcal{H}_{12}^2 - \mathcal{H}_{13}\mathcal{H}_{22}) > 0. \tag{69c}$$

Now, as with Eq. (56) for the case of $1 < p < \infty$, the inequality for $p = \infty$

$$\langle \mathrm{sgn}[\bar{Z}(\theta) + \lambda] Z''(\theta + \Delta\phi) \rangle < 0, \tag{70}$$

is derived from Eq. (69c) as follows. First, we have $\mathcal{H}_{13} > 0$ in Eq. (68b), and this implies $\mathcal{H}_{12}^2 - \mathcal{H}_{13}\mathcal{H}_{22} > 0$ from Eq. (69c). Then, we obtain

$$\mathcal{H}_{12}^2 = \left[2 \sum_{i=1}^{n} \frac{Z'(\theta_i + \Delta\phi)}{|\bar{Z}'(\theta_i)|} \right]^2, \tag{71}$$

and

$$\mathcal{H}_{13}\mathcal{H}_{22} = \left[2 \sum_{i=1}^{n} \frac{1}{|\bar{Z}'(\theta_i)|} \right] \left[2 \sum_{i=1}^{n} \frac{Z'(\theta_i + \Delta\phi)^2}{|\bar{Z}'(\theta_i)|} + \left\langle \mathrm{sgn}[\bar{Z}(\theta) + \lambda] Z''(\theta + \Delta\phi) \right\rangle \right], \tag{72}$$

respectively, from Eqs. (68a), (68b), and (68c). Using the Cauchy–Schwarz inequality, we have

$$\left[\sum_{i=1}^{n} \frac{Z'(\theta_i + \Delta\phi)}{|\bar{Z}'(\theta_i)|} \right]^2 - \left[\sum_{i=1}^{n} \frac{1}{|\bar{Z}'(\theta_i)|} \right] \left[\sum_{i=1}^{n} \frac{Z'(\theta_i + \Delta\phi)^2}{|\bar{Z}'(\theta_i)|} \right] = (X \cdot Y)^2 - |X|^2 |Y|^2 \leq 0, \tag{73}$$

where $X = \left(1/\sqrt{|\bar{Z}'(\theta_1)|}, \ldots, 1/\sqrt{|\bar{Z}'(\theta_n)|} \right)$, $Y = \left(Z'(\theta_1 + \Delta\phi)/\sqrt{|\bar{Z}'(\theta_1)|}, \ldots, Z'(\theta_n + \Delta\phi)/\sqrt{|\bar{Z}'(\theta_n)|} \right)$.

Now, subtracting Eq. (72) from Eq. (71), we find this Eq. (73) is included in $\mathcal{H}_{12}^2 - \mathcal{H}_{13}\mathcal{H}_{22}$, and hence $\left\langle \mathrm{sgn}(\bar{Z}(\theta) + \lambda) Z''(\theta + \Delta\phi) \right\rangle < 0$ is obtained from $\mathcal{H}_{12}^2 - \mathcal{H}_{13}\mathcal{H}_{22} > 0$.

Finally, to conclude the proof, it is sufficient to verify the symmetry of F_∞ and G_∞, and $(F_\infty(\Delta\phi, \lambda) = F_\infty(-\Delta\phi, -\lambda)$ and $G_\infty(\Delta\phi, \lambda) = G_\infty(-\Delta\phi, -\lambda))$, and to verify that the optimal forcing $f_{\mathrm{opt},\,\infty}$ in Eq. (32) indeed maximizes Γ at ϕ_+ and minimizes Γ at ϕ_-, similarly to the case of $1 < p < \infty$ in Section 9.1.2. Since these are carried out by following the same procedure as followed there, we omit the details here.

Thus, we are led to the same conclusion as in Section 9.1.2: $f_{\mathrm{opt},\,\infty}$ in Eq. (32) is the global optimal forcing, whose locking range becomes the largest for the best solution $(\overline{\Delta\phi_*}, \bar{\lambda}_*)$ of Eqs. (76), (77), as stated in Theorem 2. (end of the proof of Theorem 2) ■

9.3. Proof of Theorem 3

Here, we assume that $\bar{Z}(\theta) = Z(\theta+\Delta\phi) - Z(\theta)$ has a maximum and minimum at $\theta = \theta_{\max}$ and $\theta = \theta_{\min}$, respectively (assumption (ii)), and further, without loss of generality, we assume that the value of (the maximum − the minimum) $= \bar{Z}(\theta_{\max}) - \bar{Z}(\theta_{\min})$ becomes the largest at some unique value of $\Delta\phi = \Delta\phi_{\max}$ (assumption (iii)). In the first part of this proof, we construct a specific form of $f_{*,1}$ in Eq. (75) from Eq. (21) in Lemma 5. Then, in the remainder of the proof, we verify how this $f_{*,1}$ asymptotically realizes the *ideal* locking range obtained in Lemma 5.

First, notice that the assumptions in Lemma 5 are satisfied in the context of Theorem 3. Then, we start from the general form of $f_{*,1}$ as given by Eq. (21) and here we further impose the charge-balance constraint of (5) on $f_{*,1}$. Intuitively, this constraint is satisfied if $f_{*,1}$ is a pair of one positive pulse and one negative pulse. In fact, this is realized for a particular choice of λ,

$$\lambda = -\frac{1}{2}[\bar{Z}(\theta_{\max}) + \bar{Z}(\theta_{\min})], \tag{74}$$

which is such that a maximum and minimum of $g(\theta)\,(=\bar{Z}(\theta)+\lambda)$ are located at $\theta = \theta_{\max}$ and $\theta = \theta_{\min}$, respectively, for which $|g(\theta_{\min})| = |g(\theta_{\max})|$ with $g(\theta_{\max}) = -g(\theta_{\min}) = \frac{1}{2}[\bar{Z}(\theta_{\max}) - \bar{Z}(\theta_{\min})] > 0$ is satisfied in the context of Lemma 5. Thus, from Eq. (21), we obtain the precise form of $f_{*,1}$ as follows:

$$f_{*,1}(\theta) = M[\Delta(\theta - \theta_{\max}) - \Delta(\theta - \theta_{\min})], \tag{75}$$

which satisfies the charge-balance constraint.

On the other hand, from Eqs. (21) and (24) we obtain

$$\begin{aligned}\Gamma(\phi) &= \frac{1}{2\pi}\langle Z(\theta+\phi) f_{*,1}(\theta)\rangle \\ &= \frac{1}{2\pi}\langle Z(\theta+\phi) M \sum_{i=1}^{n} \mathrm{sgn}[\bar{Z}(\theta)+\lambda]\Delta(\theta-\bar{\theta}_i)\rangle \\ &\to \frac{M}{2n\pi}\sum_{i=1}^{n} \mathrm{sgn}[\bar{Z}(\bar{\theta}_i)+\lambda] Z(\bar{\theta}_i+\phi), \qquad \text{(uniformly on } S\text{)}\end{aligned} \tag{76}$$

as $\epsilon \to 0$, where the uniform convergence in Eq. (76) is obtained, for instance, if $Z(\theta+\phi)$ is locally Lipschitz continuous (assumption (i)), as proved in Appendix E as (b). Then, similarly to Eq. (76), from $f_{*,1}$ in Eq. (75) we obtain

$$\begin{aligned}\Gamma(\phi) &\to \frac{M}{4\pi}[Z(\theta_{\max}+\phi) - Z(\theta_{\min}+\phi)] \\ &\equiv \Gamma_0(\phi) \quad (\text{uniformly}, \epsilon \to 0).\end{aligned} \tag{77}$$

First, we notice that $\Gamma_0(\phi)$ in Eq. (77) has virtually the same form as $\bar{Z}(\theta) = Z(\theta+\Delta\phi) - Z(\theta)$. Namely, Γ_0 becomes

$$\Gamma_0(\bar{\phi}) = \frac{M}{4\pi}[Z(\bar{\phi}+\theta_{\max}-\theta_{\min}) - Z(\bar{\phi})] \tag{78}$$

by setting $\bar{\phi} = \phi + \theta_{\min}$, and here we can denote this $Z(\bar{\phi}+\theta_{\max}-\theta_{\min}) - Z(\bar{\phi})$ term as $\bar{Z}(\bar{\phi})$. Next, from the definition of $\bar{Z}$ (assumptions (ii) and (iii)), $\Gamma_0(\bar{\phi})\,(=\frac{M}{4\pi}\bar{Z}(\bar{\phi}))$ achieves the maximum and minimum at some $\bar{\phi} = \phi_+$ and $\bar{\phi} = \phi_-$, respectively, and the resulting locking range is given by

$$\begin{aligned}\Gamma_0(\phi_+) - \Gamma_0(\phi_-) = \frac{M}{4\pi}&[Z(\phi_+ + \theta_{\max} - \theta_{\min}) - Z(\phi_+) \\ &- \{Z(\phi_- + \theta_{\max} - \theta_{\min}) - Z(\phi_-)\}].\end{aligned} \tag{79}$$

Since this locking range is assumed to be the best one realized by the best candidate (75), from Eq. (79) $\theta_{\max} - \theta_{\min}$ should satisfy $\theta_{\max} - \theta_{\min} = \Delta\phi_{\max}$. This is because, by assumption (iii), $\theta_{\max} - \theta_{\min}$ in Eq. (79) is uniquely determined as $\Delta\phi_{\max}$ so that $\Gamma_0(\phi_+) - \Gamma(\phi_-)$ is maximized. Thus, using $\theta_{\max} - \theta_{\min} = \Delta\phi_{\max}$, we obtain Eq. (35) in Theorem 3 from Eq. (75).

So far, we have assumed the existence of the best choice of $\Delta\phi = \Delta\phi_{\max}$ and the corresponding $\theta_{\max}$ and $\theta_{\min}$. This results in a candidate for the optimal forcing (35). Now we are in position to verify that this forcing (35) realizes the *ideal* locking range $(=\frac{M}{2\pi}\|g\|_\infty)$ as $\epsilon \to +0$, as follows. First, for Eq. (35), which is equivalent to Eq. (75) with $\theta_{\max} - \theta_{\min} = \Delta\phi_{\max}$, we obtain the following, from Eq. (79) by setting $\phi_- \equiv \theta$ and $\phi_+ - \phi_- \equiv \Phi$:

$$\begin{aligned}\Gamma_0(\phi_+) - \Gamma_0(\phi_-) &= \Gamma_0(\phi_- + \Phi) - \Gamma_0(\phi_-) \\ &= \frac{M}{4\pi}[Z(\theta + \Delta\phi_{\max} + \Phi) - Z(\theta+\Phi) \\ &\quad - \{Z(\theta+\Delta\phi_{\max}) - Z(\theta)\}].\end{aligned} \tag{80}$$

Here, we use a simple property: any periodic continuous function of the form $p(\theta+\Phi) - p(\theta)$ is maximized at some θ if and only if $\Phi = \Theta_{\max} - \Theta_{\min}$, where a periodic continuous function $p(\theta)$ achieves the maximum and the minimum respectively at $\Theta_{\max}$ and $\Theta_{\min}$. From this property, $\Gamma_0(\phi_+) - \Gamma_0(\phi_-)$ is maximized at some $\theta\,(=\phi_-)$ if we set $\Phi = \theta_{\max} - \theta_{\min}$, since the above $p(\theta)$ is regarded as $Z(\theta+\Delta\phi_{\max}) - Z(\theta)$. This implies that for Eq. (35) the locking range $\Gamma_0(\phi_+) - \Gamma_0(\phi_-)$ is really maximized for certain ϕ_+ and ϕ_- satisfying $\phi_+ - \phi_- = \theta_{\max} - \theta_{\min} = \Delta\phi_{\max}$. Furthermore, this $\phi_+ - \phi_- = \theta_{\max} - \theta_{\min}$ is consistent with the assumption that $Z(\theta+\Delta\phi_{\max}) - Z(\theta)$ is maximized and minimized at $\theta = \theta_{\max}$ and $\theta = \theta_{\min}$, respectively.

Finally, $\Gamma_0(\phi_+) - \Gamma_0(\phi_-) = \frac{M}{2\pi}\|g\|_\infty$ is obtained as follows. First, by the definition of $g(\theta)$ and by $\theta_{\max} - \theta_{\min} = \Delta\phi_{\max}$, $[Z(\theta + \Delta\phi_{\max} + \theta_{\max} - \theta_{\min}) - Z(\theta + \theta_{\max} - \theta_{\min}) - \{Z(\theta + \Delta\phi_{\max}) - Z(\theta)\}] = g(\theta+\Delta\phi_{\max}) - g(\theta)$. Thus, $\Gamma_0(\phi_+) - \Gamma_0(\phi_-)$ corresponds to the maximum of $g(\theta+\Delta\phi_{\max}) - g(\theta)$, from Eq. (80). Furthermore, this maximum of $g(\theta+\Delta\phi_{\max}) - g(\theta)$ becomes $2g(\theta_{\max}) = 2\|g\|_\infty$ since $g(\theta_{\max}) = -g(\theta_{\min}) > 0$. Plugging this into Eq. (80), we obtain $\frac{M}{2\pi}\|g\|_\infty$ as the *ideal* locking range realized with $f_{*,1}$. ■

Acknowledgments

The author (H.T.) is indebted to Dr. Hayato Chiba, Dr. Hiroya Nakao, Dr. Yasuhiro Tsubo, and Dr. Kazuyuki Yoshimura for their enlightening suggestions and critical reading of the manuscript. H.T. also appreciates anonymous referees for their critical comments. This work was supported by MEXT, Japan (No. 23360047), and by the Support Center for Advanced Telecommunications Technology Research (SCAT). H.T. would like to dedicate this work to Prof. Shin'ichi Oishi in celebration of his 60th birthday.

Appendix A. Non-existence of $f_{\text{ideal},1}$

Here we prove the non-existence of $f_{\text{ideal},1}$ mentioned in Section 4.4. We make the following assumptions about $f_{\text{ideal},1}$ and g.

A1 $f_{\text{ideal},1}$ and g are measurable functions. $f_{\text{ideal},1}$ having non-zero values on an interval $I = [a, b] \subset S$. $g(\theta)$ has a maximum at $\theta = \theta_*$, at which it is continuous, *i.e.*, $|g(\theta_*)| = \|g\|_\infty$. Without loss of generality, we here set $\theta_* = 0$ and assume $a < 0 < b$. Also, for simplicity, we assume that this θ_* is unique and isolated.[4]

A2 $f_{\text{ideal},1}(\theta)$ satisfies Eq. (20), namely

$$\begin{aligned}\langle f_{\text{ideal},1}(\theta)\, g(\theta)\rangle &= \|f_{\text{ideal},1}\, g\|_1 = \|f_{\text{ideal},1}\|_1 \|g\|_\infty \\ &= M\|g\|_\infty.\end{aligned} \tag{A.1}$$

[4] Even if $g(\theta)$ has multiple, isolated maxima $\theta_{*,i}$, the argument here can be repeated to construct subinterval I_n instead of I_2, and this would lead to the same kind of contradiction as shown for the assumed case.

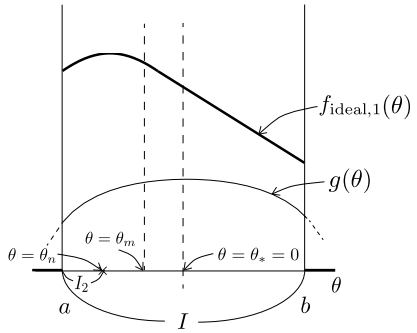

Fig. A.1. Non-existence of $f_{\text{ideal},\,1}$.

Due to the continuity of the integral $\int_a^{\theta} f_{\text{ideal},\,1}(\theta)\, g(\theta)\, d\theta$ with respect to θ, there exists $\theta_m \in I$ such that the following holds:

$$\int_a^{\theta_m} f_{\text{ideal},\,1}(\theta)\, g(\theta)\, d\theta = \int_{\theta_m}^{b} f_{\text{ideal},\,1}(\theta)\, g(\theta)\, d\theta = \frac{M}{2}\|g\|_\infty. \quad \text{(A.2)}$$

Then, focusing on this θ_m, we consider the following two cases, separately, as follows.

C1 Case of $\int_a^{\theta_m} |f_{\text{ideal},\,1}(\theta)|d\theta \neq \int_{\theta_m}^{b} |f_{\text{ideal},\,1}(\theta)|d\theta$

Having $\|f_{\text{ideal},\,1}\|_1 = \int_a^{b} |f_{\text{ideal},\,1}(\theta)|d\theta = M$ in mind, we assume $\int_{\theta_m}^{b} |f_{\text{ideal},\,1}(\theta)|d\theta < \frac{M}{2}$ without loss of generality. Then we have $\int_{\theta_m}^{b} 2f_{\text{ideal},\,1}(\theta)\, g(\theta)\, d\theta = M\|g\|_\infty$ from Eq. (A.2) and $\int_{\theta_m}^{b} |2f_{\text{ideal},\,1}(\theta)|d\theta < M$ from the above assumption. This implies the existence of a better forcing $f_*(\theta)$ defined as

$$f_*(\theta) = \begin{cases} 2Cf_{\text{ideal},\,1}(\theta) & \theta \in [\theta_m,\ b] \\ 0 & \text{otherwise,} \end{cases} \quad \text{(A.3)}$$

where $C(>1)$ satisfies $\int_{\theta_m}^{b} C|2f_{\text{ideal},\,1}(\theta)|d\theta = M$. And, it satisfies $\|f_*\|_1 = M$ and $\|f_*\, g\|_1 > M\|g\|_\infty$. However, this contradicts Hölder's inequality (20).

C2 Case of $\int_a^{\theta_m} |f_{\text{ideal},\,1}(\theta)|d\theta = \int_{\theta_m}^{b} |f_{\text{ideal},\,1}(\theta)|d\theta$

In this case, we pick the interval $[a, \theta_m]$ (or $[\theta_m, b]$) as shown in Fig. A.1 and divide it into $[a, \theta_n]$ and $[\theta_n, \theta_m]$ in such a way that

$$\int_a^{\theta_n} f_{\text{ideal},\,1}(\theta)\, g(\theta)\, d\theta = \int_{\theta_n}^{\theta_m} f_{\text{ideal},\,1}(\theta)\, g(\theta)\, d\theta = \frac{M}{2^2}\|g\|_\infty, \quad \text{(A.4)}$$

and if $\int_a^{\theta_n} |f_{\text{ideal},\,1}(\theta)|d\theta < \frac{M}{2^2}$ holds, the same argument as that for **C1** is repeated. Otherwise, if $\int_a^{\theta_n} |f_{\text{ideal},\,1}(\theta)|d\theta = \frac{M}{2^2}$ holds, this implies the existence of a subinterval $I_2 \subset I$ which does not contain $\theta = \theta_*$. As shown in Fig. A.1, we define this I_2 as $[a, \theta_n]$ without loss of generality, and this existence implies the existence of $f_*(\theta)$ having non-zero values on I_2 that satisfies $\|f_*\|_1 = M$ and $\langle |f_*(\theta)\, g(\theta)| \rangle = M\|g\|_\infty$. However, since the essential supremum of $|g(\theta)|$ on I_2 (*i.e.*, $\|g\|_{\infty,I_2}$) is less than that on S (*i.e.*, $\|g\|_\infty$), it follows that we have $\langle f_*(\theta)g(\theta) \rangle \leq \int_{I_2} |f_*(\theta)|d\theta \cdot \|g\|_{\infty,I_2} < M\|g\|_\infty$. This contradicts $\langle |f_*(\theta)g(\theta)| \rangle = M\|g\|_\infty$. ■

Appendix B. Derivation of Eqs. (46)–(49), (51c), (51d), (64)–(67), and (68c), (68d)

Here, the derivation of Eqs. (46)–(49), (51c), (51d), (64)–(67), and (68c), (68d) is outlined. For those who are familiar with the delta function, these equations can be formally derived with much less effort, for instance, by using the formula $\delta[f(x)] = \sum_i \frac{\delta(x - x_i)}{|f'(x_i)|}$, where x_i are the roots of $f(x) = 0$. However, without using such a technique, all equations can be obtained by elementary arithmetic, which seems instructive and educational, and so we outline this procedure in the following.

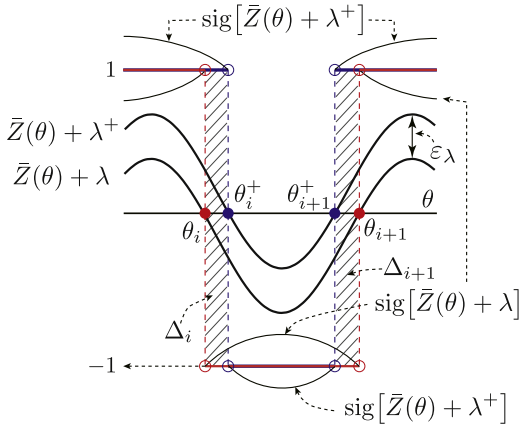

Fig. B.1. Case of the differentiation with respect to λ (for Eq. (67)).

Required calculations are classified into two cases: (i) differentiation with respect to λ, and (ii) differentiation with respect to $\Delta\phi$. These two cases are considered separately, as follows. Here we assume that $\bar{Z}(\theta)$ is twice differentiable, which is a direct consequence of assumption (i) in Theorem 1 and/or Theorem 2, and the definition of $\bar{Z}$ in Eq. (23b).

(i) Case of differentiation with respect to λ

We consider here a prototypical case of Eq. (67):

$$\frac{\partial G_\infty}{\partial \lambda} = \frac{\partial}{\partial \lambda}\langle \text{sgn}[\bar{Z}(\theta) + \lambda] \rangle = \lim_{\epsilon_\lambda \to 0} \frac{1}{\epsilon_\lambda}\left[\langle \text{sgn}[\bar{Z}(\theta) + \lambda^+] \rangle - \langle \text{sgn}[\bar{Z}(\theta) + \lambda] \rangle\right], \quad \text{(B.1)}$$

in which $\lambda^+ \equiv \lambda + \epsilon_\lambda$. The reason why we refer to this as prototypical is that this particular case includes all elements for deriving all other equations of (47), (49), (51d), (65), (67), (68d). In Eq. (B.1), $\langle \text{sgn}[\bar{Z}(\theta) + \lambda^+] \rangle - \langle \text{sgn}[\bar{Z}(\theta) + \lambda] \rangle \equiv \int_{-\pi}^{\pi} \text{sgn}[\bar{Z}(\theta) + \lambda^+]\, d\theta - \int_{-\pi}^{\pi} \text{sgn}[\bar{Z}(\theta) + \lambda]\, d\theta = \langle \text{sgn}[\bar{Z}(\theta) + \lambda^+] - \text{sgn}[\bar{Z}(\theta) + \lambda] \rangle$, and this $\text{sgn}[\bar{Z}(\theta) + \lambda^+] - \text{sgn}[\bar{Z}(\theta) + \lambda]$ is related to the regions $\Delta_i \equiv \{(\theta, h) | \theta_i \leq \theta \leq \theta_i^+,\ -1 \leq h \leq 1\}$ as shown in Fig. B.1, where θ_i and θ_i^+ respectively denote the ith roots of $\bar{Z}(\theta) + \lambda = 0$ and $\bar{Z}(\theta) + \lambda^+ = 0$. Since $\bar{Z}$ is twice differentiable, $\bar{Z}(\theta_i^+) + \lambda^+ = \bar{Z}(\theta_i) + \bar{Z}'(\theta_i)(\theta_i^+ - \theta_i) + \lambda + \epsilon_\lambda + O(\epsilon_\lambda^2) = \bar{Z}'(\theta_i)(\theta_i^+ - \theta_i) + \epsilon_\lambda + O(\epsilon_\lambda^2) = 0$ implies $\theta_i^+ - \theta_i = -\frac{\epsilon_\lambda}{\bar{Z}'(\theta_i)} + O(\epsilon_\lambda^2)$, which results in

$$|\theta_i^+ - \theta_i| = \frac{\epsilon_\lambda}{|\bar{Z}'(\theta_i)|} + O(\epsilon_\lambda^2). \quad \text{(B.2)}$$

Also, observing the above situations in Fig. B.1, we have

$$\langle \text{sgn}[\bar{Z}(\theta) + \lambda^+] - \text{sgn}[\bar{Z}(\theta) + \lambda] \rangle = \sum_i |\Delta_i| = \sum_i 2|\theta_i^+ - \theta_i|, \quad \text{(B.3)}$$

where $|\Delta_i|$ represents the area of the region Δ_i. Plugging Eq. (B.2) into Eq. (B.3) and plugging the resulting Eq. (B.3) into Eq. (B.1), we finally obtain

$$\frac{\partial G_\infty}{\partial \lambda} = 2\sum_i \frac{1}{|\bar{Z}'(\theta_i)|}, \quad \text{(B.4)}$$

which is already used in Eq. (67), (68b), and (68f).

(ii) Case of differentiation with respect to $\Delta\phi$

Now, the above procedure in (i) is repeated for another prototypical case of Eq. (66). Following this procedure, Eqs. (46),

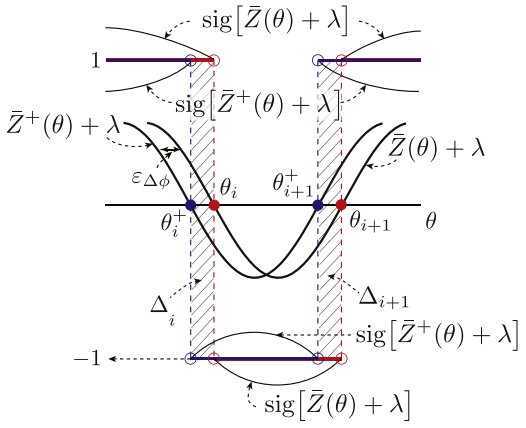

Fig. B.2. Case of the differentiation with respect to $\Delta\phi$ (for Eq. (66)).

(48), (51c), (64), and (68c) are obtained. In this case, in contrast to Eq. (B.1), we start from

$$\frac{\partial G_\infty}{\partial\Delta\phi} = \frac{\partial}{\partial\Delta\phi}\langle \mathrm{sgn}[\bar{Z}(\theta)+\lambda]\rangle$$
$$= \lim_{\epsilon_{\Delta\phi}\to 0}\frac{1}{\epsilon_{\Delta\phi}}\Big[\langle \mathrm{sgn}[\bar{Z}^+(\theta)+\lambda]\rangle - \langle \mathrm{sgn}[\bar{Z}(\theta)+\lambda]\rangle\Big], \tag{B.5}$$

in which $\bar{Z}^+(\theta)\equiv Z(\theta+\Delta\phi+\epsilon_{\Delta\phi})-Z(\theta)$. Similarly to the case of Eq. (B.3), by observing the situations in Fig. B.2, we have

$$\langle \mathrm{sgn}[\bar{Z}^+(\theta)+\lambda]\rangle - \langle \mathrm{sgn}[\bar{Z}(\theta)+\lambda]\rangle$$
$$= \langle \mathrm{sgn}[\bar{Z}(\theta)+\lambda+\epsilon_{\Delta\phi}Z'(\theta+\Delta\phi)+O(\epsilon^2_{\Delta\phi})]$$
$$- \mathrm{sgn}[\bar{Z}(\theta)+\lambda]\rangle = \sum_i D_i, \tag{B.6}$$

where D_i is defined by

$$D_i \equiv \begin{cases} \displaystyle\int_{\theta_i^+}^{\theta_i} 2\,\mathrm{sgn}[\bar{Z}'(\theta_i)]\,d\theta = 2\,\mathrm{sgn}[\bar{Z}'(\theta_i)](\theta_i-\theta_i^+), \\ \qquad \text{if } \theta_i^+ < \theta_i \\ \displaystyle\int_{\theta_i}^{\theta_i^+} -2\,\mathrm{sgn}[\bar{Z}'(\theta_i)]\,d\theta = 2\,\mathrm{sgn}[\bar{Z}'(\theta_i)](\theta_i-\theta_i^+), \\ \qquad \text{if } \theta_i < \theta_i^+ \end{cases} \tag{B.7}$$

and θ_i and θ_i^+ represent the roots of $\bar{Z}(\theta)+\lambda=0$ and $\bar{Z}^+(\theta)+\lambda=0$, respectively.

On the other hand, similarly to Eq. (B.2), $\theta_i^+-\theta_i$ is estimated as follows. From $\bar{Z}^+(\theta_i^+)+\lambda=0$, we have

$$\bar{Z}^+(\theta_i^+)+\lambda = Z(\theta_i^+ +\Delta\phi)+\epsilon_{\Delta\phi}Z'(\theta_i^+ +\Delta\phi)$$
$$+O(\epsilon^2_{\Delta\phi}) - Z(\theta_i^+)+\lambda$$
$$= Z(\theta_i+\Delta\phi)+(\theta_i^+-\theta_i)Z'(\theta_i+\Delta\phi)+O(\epsilon^2_{\Delta\phi})$$
$$+\epsilon_{\Delta\phi}[Z'(\theta_i+\Delta\phi)+(\theta_i^+-\theta_i)Z''(\theta_i+\Delta\phi)+O(\epsilon^2_{\Delta\phi})]$$
$$+O(\epsilon^2_{\Delta\phi}) - [Z(\theta_i)+(\theta_i^+-\theta_i)Z'(\theta_i)+O(\epsilon^2_{\Delta\phi})]+\lambda$$
$$= (\theta_i^+-\theta_i)[Z'(\theta_i+\Delta\phi)-Z'(\theta_i)]+\epsilon_{\Delta\phi}Z'(\theta_i+\Delta\phi)$$
$$+\bar{Z}(\theta_i)+\lambda+O(\epsilon^2_{\Delta\phi})=0, \tag{B.8}$$

and from $\bar{Z}(\theta_i)+\lambda=0$, Eq. (B.8) implies

$$\theta_i-\theta_i^+ = \epsilon_{\Delta\phi}\frac{Z'(\theta_i+\Delta\phi)}{\bar{Z}'(\theta_i)}+O(\epsilon^2_{\Delta\phi}). \tag{B.9}$$

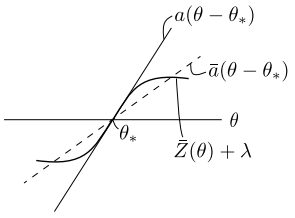

Fig. D.1. $\bar{Z}(\theta)+\lambda$ in the neighborhood of θ_*.

Plugging Eq. (B.9) into Eq. (B.7) and plugging the resulting Eq. (B.7) into Eq. (B.6) and then into Eq. (B.5), we obtain

$$\frac{\partial G_\infty}{\partial\Delta\phi} = 2\sum_i \frac{Z'(\theta_i+\Delta\phi)}{|\bar{Z}'(\theta_i)|}, \tag{B.10}$$

which is used in Eqs. (66), (68a), and (68e).

All other equations are obtained analogously, and their derivation is omitted here.

Appendix C. Derivation of the inequality (56)

Here we describe how the inequality (56) is derived from $|\mathcal{H}(H)|>0$ in Eq. (55). From Eqs. (51) and (52), $|\mathcal{H}(H)|$ is obtained as

$$|\mathcal{H}(H)| = \mathcal{H}_{13}(\alpha\mathcal{H}_{12}^2 - \mathcal{H}_{13}\mathcal{H}_{22})$$
$$= \alpha\mathcal{H}_{13}\Big[\beta\Big(\beta\left\langle|\bar{Z}+\lambda|^{\beta-1}Z'\right\rangle^2 - \beta\left\langle|\bar{Z}+\lambda|^{\beta-1}\right\rangle$$
$$\times\left\langle|\bar{Z}+\lambda|^{\beta-1}(Z')^2\right\rangle\Big)$$
$$-\beta\left\langle|\bar{Z}+\lambda|^{\beta-1}\right\rangle\left\langle\mathrm{sgn}[\bar{Z}+\lambda]|\bar{Z}+\lambda|^{\beta}Z''\right\rangle\Big], \tag{C.1}$$

where $\bar{Z}$, Z', and Z'' respectively represent $Z(\theta+\Delta\phi)-Z(\theta)$, $Z'(\theta+\Delta\phi)$, and $Z''(\theta+\Delta\phi)$.

In Eq. (C.1), the first term plus the second term becomes non-positive:

$$\left\langle|\bar{Z}+\lambda|^{\beta-1}Z'\right\rangle^2 - \left\langle|\bar{Z}+\lambda|^{\beta-1}\right\rangle\left\langle|\bar{Z}+\lambda|^{\beta-1}(Z')^2\right\rangle \le 0, \tag{C.2}$$

since we have

$$\left\langle|\bar{Z}+\lambda|^{\beta-1}Z'\right\rangle^2 = \left\langle|\bar{Z}+\lambda|^{\frac{\beta-1}{2}}|\bar{Z}+\lambda|^{\frac{\beta-1}{2}}Z'\right\rangle^2$$
$$\le \left\langle|\bar{Z}+\lambda|^{\beta-1}\right\rangle\left\langle|\bar{Z}+\lambda|^{\beta-1}(Z')^2\right\rangle \tag{C.3}$$

from the Cauchy–Schwarz inequality.

On the other hand, in the third term of Eq. (C.1), $\left\langle|\bar{Z}+\lambda|^{\beta-1}\right\rangle$ is positive. Thus, since $\mathcal{H}_{13}>0$ and we have assumed $|\mathcal{H}(H)|>0$, the inequality (56) $\langle\mathrm{sgn}(\bar{Z}+\lambda)|\bar{Z}+\lambda|^{\beta}Z''\rangle<0$ has to be satisfied.

Appendix D. Evaluation of singular integrals in Eq. (49)

Here, we show that all the integrals involving $|\bar{Z}(\theta)+\lambda|^{\beta-1}$ in Eq. (49) have finite values if $\bar{Z}(\theta)$ is a C^2 function (and hence locally Lipschitz continuous) and $\bar{Z}'(\theta_*)\neq 0$.

First, we assume $\bar{Z}'(\theta_*)=a>0$, without loss of generality. Then, in the ϵ-neighborhood of θ_*, there exists $0<\bar{a}<a$ such that $|\bar{a}(\theta-\theta_*)|<|\bar{Z}(\theta)+\lambda|$ holds, as shown in Fig. D.1, since $\bar{Z}(\theta_*)+\lambda=0$ and $\beta-1<0$. Thus, we obtain the following estimate:

$$\int_{\theta_*-\epsilon}^{\theta_*+\epsilon}|\bar{Z}(\theta)+\lambda|^{\beta-1}d\theta < \int_{\theta_*-\epsilon}^{\theta_*+\epsilon}|\bar{a}(\theta-\theta_*)|^{\beta-1}d\theta$$
$$= \bar{a}^{\beta-1}2\int_{\theta_*}^{\theta_*+\epsilon}(\theta-\theta_*)^{\beta-1}d\theta = \frac{2}{\beta}\bar{a}^{\beta-1}\epsilon^{\beta}. \tag{D.1}$$

Also, the following inequality holds:

$$m\int_{\theta_*-\epsilon}^{\theta_*+\epsilon}|\bar{Z}(\theta)+\lambda|^{\beta-1}d\theta < \int_{\theta_*-\epsilon}^{\theta_*+\epsilon}|\bar{Z}(\theta)+\lambda|^{\beta-1}Z'(\theta+\Delta\phi)d\theta < M\int_{\theta_*-\epsilon}^{\theta_*+\epsilon}|\bar{Z}(\theta)+\lambda|^{\beta-1}d\theta, \quad \text{(D.2)}$$

where $m(<0)$ and $M(>0)$ are respectively the minimum and the maximum of $Z'(\theta+\Delta\phi)$ for $\theta \in S$. Using the estimate Eq. (D.1), we obtain from Eq. (D.2)

$$m\frac{2}{\beta}\bar{a}^{\beta-1}\epsilon^{\beta} < \int_{\theta_*-\epsilon}^{\theta_*+\epsilon}|\bar{Z}(\theta)+\lambda|^{\beta-1}Z'(\theta+\Delta\phi)d\theta < M\frac{2}{\beta}\bar{a}^{\beta-1}\epsilon^{\beta}. \quad \text{(D.3)}$$

Similarly to Eq. (D.3), the same kind of inequality is obtained for

$$\int_{\theta_*-\epsilon}^{\theta_*+\epsilon}|\bar{Z}(\theta)+\lambda|^{\beta-1}Z'(\theta+\Delta\phi)^2d\theta. \quad \text{(D.4)}$$

From the above estimates, all the integrals in Eqs. (D.1)–(D.3) are $O(\epsilon^{\beta})$ and they have finite values for sufficiently small ϵ. ■

Appendix E. Proofs of $\langle f_{*,1}g\rangle \to M|g(\bar{\theta}_i)|$, and Eq. (76)

(a) Proof for $\langle f_{*,1}g\rangle = M\langle\sum_{i=1}^{n}\mathrm{sgn}[g(\bar{\theta}_i)]\Delta(\theta-\bar{\theta}_i)g(\theta)\rangle \to M|g(\bar{\theta}_i)|$ $(\epsilon\to+0)$

By the assumption, all $\bar{\theta}_i$ are isolated from each other, and g is continuous at each $\bar{\theta}_i$, and $\|g\|_\infty = |g(\bar{\theta}_i)| = |g(\bar{\theta}_j)|$. Also, from the definition of Δ in Eq. (22),

$$\left\langle\sum_{i=1}^{n}\mathrm{sgn}[g(\bar{\theta}_i)]\Delta(\theta-\bar{\theta}_i)g(\theta)\right\rangle = \sum_{i=1}^{n}\left\langle\mathrm{sgn}[g(\bar{\theta}_i)]\Delta(\theta-\bar{\theta}_i)g(\theta)\right\rangle. \quad \text{(E.1)}$$

Since g is continuous at each isolated $\bar{\theta}_i$, it is safely assumed that for sufficiently small ϵ, $g(\theta) > 0$ (or $g(\theta) < 0$) is satisfied for any $\theta \in [\bar{\theta}_i-\epsilon, \bar{\theta}_i+\epsilon] \equiv I_\epsilon$, and $\left\langle\mathrm{sgn}[g(\bar{\theta}_i)]\Delta(\theta-\bar{\theta}_i)g(\theta)\right\rangle = \langle\Delta(\theta-\bar{\theta}_i)|g(\theta)|\rangle$ is immediate. As g is continuous on I_ϵ, if there exists a minimum of g at $\theta=\theta_{\min}$ in I_ϵ as well as a maximum at $\theta=\bar{\theta}_i$ in I_ϵ, then the following estimate is obtained:

$$\frac{1}{2n\epsilon}2\epsilon|g(\theta_{\min})| \le \langle\Delta(\theta-\bar{\theta}_i)|g(\theta)|\rangle \le \frac{1}{2n\epsilon}2\epsilon|g(\bar{\theta}_i)|. \quad \text{(E.2)}$$

Now, $\theta_{\min}\to\bar{\theta}_i$ $(\epsilon\to0)$ since g is continuous in I_ϵ. Therefore,

$$\langle\Delta(\theta-\bar{\theta}_i)|g(\theta)|\rangle \to \frac{1}{2n\epsilon}2\epsilon|g(\bar{\theta}_i)| = \frac{1}{n}\left|g(\bar{\theta}_i)\right|. \quad \text{(E.3)}$$

Then, by summing up Eq. (E.3) over i and multiplying by M, we have $\langle f_{*,1}g\rangle = M\langle\sum_{i=1}^{n}\mathrm{sgn}[g(\bar{\theta}_i)]\Delta(\theta-\bar{\theta}_i)g(\theta)\rangle \to M|g(\theta_*)|$. ■

(b) Proof of Eq. (76)

We begin by proving the following:

$$\langle Z(\theta+\phi)\Delta(\theta-\bar{\theta}_i)\rangle \to \frac{1}{n}Z(\bar{\theta}_i+\phi). \quad \text{(uniformly for } \phi\in S,\ \epsilon\to0). \quad \text{(E.4)}$$

Here we assume that Z is locally Lipschitz continuous and that the Lipschitz constant is given as k. Then, $\langle Z(\theta+\phi)\Delta(\theta-\bar{\theta}_i)\rangle - \frac{1}{n}Z(\bar{\theta}_i+\phi)$ is evaluated as

$$\begin{aligned}&\langle Z(\theta+\phi)\Delta(\theta-\bar{\theta}_i)\rangle - \frac{1}{n}Z(\bar{\theta}_i+\phi)\\ &= \int_{\theta\in[\bar{\theta}_i-\epsilon,\ \bar{\theta}_i+\epsilon]}Z(\theta+\phi)\Delta(\theta-\bar{\theta}_i) - \frac{1}{2\epsilon\cdot n}Z(\bar{\theta}_i+\phi)d\theta\\ &= \int_{\theta\in[\bar{\theta}_i-\epsilon,\ \bar{\theta}_i+\epsilon]}\frac{1}{2n\epsilon}[Z(\theta+\phi)-Z(\bar{\theta}_i+\phi)]d\theta\\ &< \frac{1}{2n\epsilon}\cdot k\epsilon^2, \end{aligned} \quad \text{(E.5)}$$

since $|Z(\theta+\phi)-Z(\bar{\theta}_i+\phi)| < k|\theta-\bar{\theta}_i|$ $(\forall\phi\in S)$. Likewise, $\langle Z(\theta+\phi)\Delta(\theta-\bar{\theta}_i)\rangle - \frac{1}{n}Z(\bar{\theta}_i+\phi) > -\frac{1}{2n\epsilon}\cdot k\epsilon^2$ is obtained. Therefore, $\sup_{\phi\in S}\left|\left\langle Z(\theta+\phi)\Delta(\theta-\bar{\theta}_i)\right\rangle - \frac{1}{n}Z(\bar{\theta}_i+\phi)\right| \to 0$ $(\epsilon\to0)$ follows. ■

Appendix F. Continuity of derivatives $\frac{\partial H}{\partial\Delta\phi}$, $\frac{\partial H}{\partial\lambda}$, $\frac{\partial^2 H}{\partial\Delta\phi^2}$, $\frac{\partial^2 H}{\partial\Delta\phi\partial\lambda}$, $\frac{\partial^2 H}{\partial\lambda\partial\Delta\phi}$, and $\frac{\partial^2 H}{\partial\lambda^2}$

Here the continuity of several derivatives of H is verified. Since these derivatives of H are explicitly given in Eq. (51), their continuity is directly verified using the (ϵ,δ)-definition of limit, taking care of the contributions from singular integrals in Eq. (51). For instance, the continuity of $\frac{\partial^2 H}{\partial\lambda^2}$ is verified as follows. Note that the continuity of other derivatives is verified analogously, using the expressions in Eq. (51) and the results in Appendix E. Since $\frac{\partial^2 H}{\partial\lambda^2}$ is given by $\mathcal{H}_{33}(\Delta\phi,\lambda)$ in Eq. (51f), the following estimate is obtained:

$$\begin{aligned}&|\mathcal{H}_{33}(\Delta\phi,\lambda+\delta)-\mathcal{H}_{33}(\Delta\phi,\lambda)|\\ &= |\alpha\beta\langle|Z(\theta+\Delta\phi)-Z(\theta)+\lambda\\ &\quad+\delta|^{\beta-1}-|Z(\theta+\Delta\phi)-Z(\theta)+\lambda|^{\beta-1}\rangle_{\bar{\epsilon}\text{-neighborhood of }\bar{\theta}_*}\\ &\quad+\alpha\beta\langle|Z(\theta+\Delta\phi)-Z(\theta)+\lambda+\delta|^{\beta-1}\\ &\quad-|Z(\theta+\Delta\phi)-Z(\theta)+\lambda|^{\beta-1}\rangle_{S\setminus\bar{\epsilon}\text{-neighborhood of }\bar{\theta}_*}|\\ &< C_1\bar{\epsilon}^{\beta}+C_2\epsilon < C\epsilon, \end{aligned} \quad \text{(F.1)}$$

where the contribution from the $\bar{\epsilon}$-neighborhood of $\bar{\theta}_*$ is of $O(\bar{\epsilon}^{\beta})$ as shown in Appendix E, and the contribution from the other part (the $S\setminus\bar{\epsilon}$-neighborhood of $\bar{\theta}_*$) can be set arbitrarily small ($C_2\epsilon$ in Eq. (F.1)) since the integrand is continuous. Thus, setting $\bar{\epsilon}^{\beta}$ as ϵ in Eq. (F.1), the desired property is verified, *i.e.*, $\forall\epsilon\ \exists\delta$ such that $|\mathcal{H}_{33}(\Delta\phi,\lambda+\delta)-\mathcal{H}_{33}(\Delta\phi,\lambda)| < C\epsilon$. ■

References

[1] A.S. Pikovsky, M.G. Rosenblum, J. Kurths, Synchronization: A Universal Concept in Nonlinear Sciences, Cambridge University Press, Cambridge, 2001.
[2] A.T. Winfree, The Geometry of Biological Time, Springer-Verlag, New York, 1980.
[3] L. Glass, Cardiac arrhythmias and circle maps: A classical problem, Chaos 1 (1991) 13–19.
[4] J.C. Jackson, J.F. Windmill, V.G. Pook, D. Robert, Synchrony through twice-frequency forcing for sensitive and selective auditory processing, Proc. Natl. Acad. Sci. 106 (2009) 10177–10182.
[5] B. van der Pol, Forced oscillations in a circuit with nonlinear resistance (reception with reactive triode), Philos. Mag. 3 (13) (1927) 65–80.
[6] R.A. Adler, Study of locking phenomena in oscillators, Proc. IRE 34 (6) (1946) 351–357.
[7] K. Takano, M. Motoyoshi, M. Fujishima, 4.8 GHz CMOS frequency multiplier with subharmonic pulse-injection locking, 2007 IEEE Asian Solid-State Circuits Conference (2007) 336–338.
[8] J. Moehlis, E. Shea-Brown, H. Rabitz, Optimal inputs for phase models of spiking neurons, ASME J. Comput. Nonlinear Dynam. 1 (4) (2006) 358–367.
[9] I. Dasanayake, J.-S. Li, Optimal design of minimum-power stimuli for phase models of neuon oscillators, Phys. Rev. E 83 (2011) 061916.
[10] X.L. Feng, C.J. White, A. Hajimiri, M.L. Roukes, A self-sustaining ultrahigh-frequency nanoelectromechanical oscillator, Nat. Nanotechnol. 3 (2008) 342–346.

[11] M.C. Cross, A. Zumdieck, R. Lifshitz, J.L. Rogers, Synchronization by nonlinear frequency pulling, Phys. Rev. Lett. 93 (2004) 224101.
[12] K. Kawasaki, Y. Akiyama, K. Komori, M. Uno, H. Takeuchi, T. Itagaki, Y. Hino, Y. Kawasaki, K. Ito, A. Hajimiri, A millimeter-wave intra-connect solution, ISSCC Dig. Tech. Pap. (2010) 414–415.
[13] O. Mondragón-Palomino, T. Danino, J. Selimkhanov, L. Tsimring, J. Hasty, Entrainment of a population of synthetic genetic oscillators, Science 333 (2011) 1315–1319.
[14] Y. Kuramoto, Chemical Oscillations, Waves and Turbulence, Springer, Berlin, 1984.
[15] F.C. Hoppensteadt, E.M. Izhikevich, Weakly Connected Neural Networks, Springer, New York, 1997.
[16] A.E. Granada, H. Herzel, How to achieve fast entrainment? The timescale to synchronization, PLoS One 4 (2009) e7057.
[17] A. Zlotnik, Y. Chen, I.Z. Kiss, H.-A. Tanaka, J.-S. Li, Optimal waveform for fast entrainment of weakly forced nonlinear oscillators, Phys. Rev. Lett. 111 (2013) 024102.
[18] N. Bagheri, J. Stelling, F.J. Doyle, Circadian phase resetting via single and multiple control targets, PLoS Comput. Biol. 4 (2008) e1000104.
[19] D. Forger, D. Paydarfar, Starting, stopping, and resetting biological oscillators: In search of optimum perturbations, J. Theoret. Biol. 230 (2004) 521.
[20] D. Lebiedz, S. Sager, H.G. Bock, P. Lebiedz, Annihilation of limit-cycle oscillations by identification of critical perturbing stimuli via mixed-integer optimal control, Phys. Rev. Lett. 95 (2005) 108303.
[21] V. Gintautas, A.W. Hübler, Resonant forcing of nonlinear systems of differential equations, Chaos 18 (3) (2008) 033118.
[22] A. Nabi, J. Moehlis, Time optimal control of spiking neurons, J. Math. Biol. 64 (2012) 981–1004.
[23] J. Ritt, Evaluation of entrainment of a nonlinear neural oscillator to white noise, Phys. Rev. E 68 (2003) 041915.
[24] J. Feng, H.C. Tuckwell, Optimal control of neuronal activity, Phys. Rev. Lett. 91 (2003) 018101.
[25] T. Harada, H.-A. Tanaka, M.J. Hankins, I.Z. Kiss, Optimal waveform for the entrainment of a weakly forced oscillator, Phys. Rev. Lett. 105 (2010) 088301.
[26] I.M. Gelf, S.V. Fomin, Calculus of Variations, Dover, New York, 2000, (Chapter 1).
[27] D.E. Kirk, Optimal Control Theory: An Introduction, Prentice-Hall, New Jersey, 1970.
[28] B. Ermentrout, Type I membranes, phase resetting curves, and synchrony, Neural Comput. 8 (1996) 988.
[29] W. Rudin, Real and Complex Analysis, third ed., McGraw-Hill, New York, 1987, pp. 63–65.
[30] H.-A. Tanaka, Synchronization limit of weakly forced nonlinear oscillators, Fast Track Communication in J. Phys. A. (2014) Accepted.
[31] J.R. Magnus, H. Neudecker, Matrix Differential Calculus with Applications in Statistics and Econometrics, revised ed., Wiley, Chichester, 1999.
[32] G.H. Hardy, J.E. Littlewood, G. Pólya, Inequalities, second ed., Cambridge University Press, Cambridge, 1988, (Chapter 7).
[33] I.Z. Kiss, Y. Zhai, private communications (2012).
[34] Y. Kawamura, H. Nakao, K. Arai, H. Kori, Y. Kuramoto, Collective phase sensitivity, Phys. Rev. Lett. 101 (2008) 024101.
[35] H. Kori, Y. Kawamura, H. Nakao, K. Arai, Y. Kuramoto, Collective-phase description of coupled oscillators with general network structure, Phys. Rev. E 80 (2009) 036207.
[36] Y. Kawamura, H. Nakao, Y. Kuramoto, Collective phase description of globally coupled excitable elements, Phys. Rev. E 84 (2011) 046211.
[37] T.W. Ko, G.B. Ermentrout, Phase-response curves of coupled oscillators, Phys. Rev. E 79 (2009) 016211.
[38] Z. Levnajić, A. Pikovsky, Phase resetting of collective rhythm in ensembles of oscillators, Phys. Rev. E 82 (2010) 056202.
[39] A. Abouzeid, G.B. Ermentrout, Type-II phase resetting curve is optimal for stochastic synchrony, Phys. Rev. E 80 (2009) 011911.
[40] S. Hata, K. Arai, R.F. Galán, H. Nakao, Optimal phase response curves for stochastic synchronization of limit-cycle oscillators by common Poisson noise, Phys. Rev. E 84 (2011) 016229.
[41] D.S. Goldobin, J.-n. Teramae, H. Nakao, G.B. Ermentrout, Dynamics of limit cycle oscillators subject to general noise, Phys. Rev. Lett. 105 (2010) 154101.
[42] H. Nakao, T. Yanagita, Y. Kawamura, Phase description of stable limit-cycle solutions in reaction–diffusion systems, Procedia IUTAM 5 (2012) 227–233.
[43] Z.P. Kilpatrick, G.B. Ermentrout, Response of traveling waves to transient inputs in neural fields, Phys. Rev. E 85 (2012) 021910.
[44] T. Hikihara, Y. Okamoto, Y. Ueda, An experimental spatio-temporal state transition of coupled magneto-elastic system, Chaos 7 (1997) 810–816.
[45] M. Sato, B.E. Hubbard, A.J. Sievers, B. Ilic, D.A. Czaplewski, H.G. Craighead, Observation of locked intrinsic localized vibrational modes in a micromechanical oscillator array, Phys. Rev. Lett. 90 (2003) 044102.
[46] M. Sato, B.E. Hubbard, A.J. Sievers, B. Ilic, H.G. Craighead, Optical manipulation of intrinsic localized vibrational energy in cantilever arrays, Europhys. Lett. 66 (2004) 318–323.
[47] R.S. MacKay, S. Aubry, Proof of existence of breathers for time-reversible or Hamiltonian networks of weakly coupled oscillators, Nonlinearity 7 (1994) 1623–1643.
[48] M. Sato, A.J. Sievers, Experimental and numerical exploration of intrinsic localized modes in an atomic lattice, J. Biol. Phys. 35 (2009) 57–72.